AD/A-004 098

INVESTIGATION OF SURFACE TENSION SCREENS FOR USE IN RAMJET FUEL SYSTEMS

Jack R. Fultz

Air Force Aero Propulsion Laboratory
Wright-Patterson Air Force Base, Ohio

October 1974

DISTRIBUTED BY:

NTIS
National Technical Information Service
U. S. DEPARTMENT OF COMMERCE

UNCLASSIFIED
Security Classification

AD/A-004098

DOCUMENT CONTROL DATA - R & D

(Security classification of title, body of abstract and indexing annotation must be entered when the overall report is classified)

1. ORIGINATING ACTIVITY *(Corporate author)* Air Force Aero Propulsion Laboratory Wright-Patterson Air Force Base, Ohio 45433	2a. REPORT SECURITY CLASSIFICATION Unclassified 2b. GROUP

3. REPORT TITLE

INVESTIGATION OF SURFACE TENSION SCREENS FOR USE IN RAMJET FUEL SYSTEMS

4. DESCRIPTIVE NOTES *(Type of report and inclusive dates)*

Final report January 1973 through July 1973

5. AUTHOR(S) *(First name, middle initial, last name)*

Jack R. Fultz

6. REPORT DATE October 1974	7a. TOTAL NO. OF PAGES 69	7b. NO. OF REFS 8
8a. CONTRACT OR GRANT NO. b. PROJECT NO. 3012 c. Task 301211 d. Work Unit 30121103	9a. ORIGINATOR'S REPORT NUMBER(S) AFAPL-TR-74-29 9b. OTHER REPORT NO(S) *(Any other numbers that may be assigned this report)*	

10. DISTRIBUTION STATEMENT

Approved for public release; distribution unlimited.

11. SUPPLEMENTARY NOTES	12. SPONSORING MILITARY ACTIVITY Air Force Aero Propulsion Laboratory (RJA) Wright-Patterson Air Force Base, Ohio 45433

13. ABSTRACT

This report presents an analysis of surface tension screens for their applicability to fuel systems in ramjet-powered vehicles. Selection of surface tension screens for fuel expulsion over other expulsion techniques was made on the basis of their high temperature capability, moderate pressure requirements, geometrical considerations, simplicity (no moving parts), and other factors. Analysis of the pressure losses encountered in expelling the heavy hydrocarbon fuel (RJ-5) used in this study revealed that the primary pressure loss in the system was encountered in flowing the fuel through the surface tension screen. The time required to expell fuel from various trap tank sizes was calculated as a function of fuel flow rate. Parameter investigated in addition to trap tank size included orifice vent area and acceleration (g's) force. Results of this analysis revealed that large pressure drops were encountered in flowing the RJ-5 fuel through surface tension screens having sufficiently small holes to provide appreciable surface tension force. The primary reason for this large pressure drop is the high viscosity of the RJ-5 fuel. The utility of surface tension screens for ramjet fuel systems using RJ-5 fuel is limited to high fuel temperatures at low (∿3) acceleration (g's) level. If low viscosity blends of high density fuels are developed and further analysis reveals that low g operation is feasible during the critical fuel expulsion cycle, then a more detailed analysis of surface tension screens for ramjet-powered vehicles will be warranted.

i

PRICES SUBJECT TO CHANGE

DD FORM 1 NOV 65 1473

Reproduced by
NATIONAL TECHNICAL
INFORMATION SERVICE
U S Department of Commerce
Springfield VA 22151

UNCLASSIFIED
Security Classification

UNCLASSIFIED
Security Classification

14. KEY WORDS	LINK A ROLE	LINK A WT	LINK B ROLE	LINK B WT	LINK C ROLE	LINK C WT
Surface Tension Screens						
Fuel Systems						
Ramjet Fuel System						
Heavy Hydrocarbon Fuel (RJ-5) Expulsion						

UNCLASSIFIED
Security Classification

☆U.S.Government Printing Office: 1974 — 657-017/352

NOTICE

When Government drawings, specifications, or other data are used for any purpose other than in connection with a definitely related Government procurement operation, the United States Government thereby incurs no responsibility nor any obligation whatsoever; and the fact that the government may have formulated, furnished, or in any way supplied the said drawings, specifications, or other data, is not to be regarded by implication or otherwise as in any manner licensing the holder or any other person or corporation, or conveying any rights or permission to manufacture, use, or sell any patented invention that may in any way be related thereto.

ACCESSION for
NTIS White Section ☑
DDC Buff Section ☐
UNANNOUNCED ☐
JUSTIFICATION .....
BY .....
DISTRIBUTION/AVAILABILITY CODES
Dist. AVAIL. and/or SPECIAL
A

Copies of this report should not be returned unless return is required by security considerations, contractual obligations, or notice on a specific document.

AIR FORCE/56780/21 January 1975 — 150

AFAPL-TR-74-29

INVESTIGATION OF SURFACE TENSION SCREENS FOR USE IN RAMJET FUEL SYSTEMS

Jack R. Fultz

Approved for public release; distribution unlimited.

ib

FOREWORD

This report describes an analytical investigation of the applicability of surface tension screens for use in ramjet fuel systems using the heavy hydrocarbon fuel RJ-5. The analysis was performed in the Air Force Aero Propulsion Laboratory, Wright-Patterson Air Force Base, Ohio by Jack R. Fultz (RJA). The work was performed under Project 3012, "Ramjet Technology", Task 301211, "Ramjet Design and Assessment", Work Unit Number 30121103, "Multi-Purpose Missile Design Studies" during the period January 1973 through July 1973.

This report was submitted by the author April 1974.

This technical report has been reviewed and is approved.

Earl D. Payne

EARL D. PAYNE, Chief
Ramjet Applications Branch
Ramjet and Laser Aerodynamics
Division
AF Aero Propulsion Laboratory

ABSTRACT

This report presents an analysis of surface tension screens for their applicability to fuel systems in ramjet-powered vehicles. Selection of surface tension screens for fuel expulsion over other expulsion techniques was made on the basis of their high temperature capability, moderate pressure requirements, geometrical considerations, simplicity (no moving parts), and other factors. Analysis of the pressure losses encountered in expelling the heavy hydrocarbon fuel (RJ-5) used in this study revealed that the primary pressure loss in the system was encountered in flowing the fuel through the surface tension screen. The time required to expell fuel from various trap tank sizes was calculated as a function of fuel flow rate. Parameters investigated in addition to trap tank size included orifice vent area and acceleration (g's) force. Result of this analysis revealed that large pressure drops were encountered in flowing the RJ-5 fuel through surface tension screens having sufficiently small holes to provide appreciable surface tension force. The primary reason for this large pressure drop is the high viscosity of the RJ-5 fuel. The utility of surface tension screens for ramjet fuel systems using RJ-5 fuel is limited to high fuel temperatures at low ($\sim$3) acceleration (g's) level. If low viscosity blends of high density fuels are developed and further analysis reveals that low g operation is feasible during the critical fuel expulsion cycle, then a more detailed analysis of surface tension screens for ramjet-powered vehicles will be warranted.

TABLE OF CONTENTS

SECTION		PAGE
I	INTRODUCTION	1
II	PRIMARY DESIGN PARAMETERS	9
III	TRAP TANK SIZING	25
IV	CONCLUSIONS AND RECOMMENDATIONS	50
APPENDIX - CALCULATION TECHNIQUE FOR TRAP TANK SIZING		51
REFERENCES		58

Preceding page blank

LIST OF ILLUSTRATIONS

FIGURE		PAGE
1.	Candidate Expulsion Techniques	2
2.	Hydrodynamic Regimes	6
3.	Operation Principle of Surface Tension Screens	10
4.	Retention Capability of Surface Tension Screens	15
5.	Screen Discharge Coefficients for Surface Tension Screens	18
6.	Surface Tension Screens Pressure Drops	20
7.	Trap Tank Flow Model	27
8.	Trap Tank Schematic	28
9.	Trap Tank Fuel Volume Versus Fuel Height for 9 Inch Tank	31
10.	Trap Tank Fuel Volume Versus Fuel Height for 3.2 Inch Tank	33
11.	Tank Emptying Time, 9 Inch Height, 9 Inch Length, 10 G's, Various Vent Areas	35
12.	Tank Emptying Time, 9 Inch Height, 9 Inch Length, 0.20 In^2 Vent Area, Various G Levels	37
13.	Tank Emptying Time, 6 Inch Height, 9 Inch Length, 10 G's Various Vent Areas	38
14.	Tank Emptying Time, 6 Inch Height, 9 Inch Length 0.20 In^2 Vent Area, Various G Levels	40
15.	Tank Emptying Time, 9 Inch Height, 12 Inch Length, 10 G's, Various Vent Areas	41
16.	Tank Emptying Time, 9 Inch Height, 12 Inch Length, 0.20 In^2 Vent Area, Various G Levels	42
17.	Tank Emptying Time, 9 Inch Height, 10 G's, 0.20 In^2 Vent Area, Various Tank Lengths	43
18.	Tank Emptying Time, 3.2 Inch Height, 16 Inch Length, 10 G's, 0.10 and 0.20 In^2 Vent Areas	45

LIST OF ILLUSTRATIONS (Cont'd)

FIGURE		PAGE
19.	Tank Emptying Time, 3.2 Inch Height, 16 Inch Length, 10 G's, 0.15 and 0.30 In^2 Vent Areas	46
20.	Tank Emptying Time, 3.2 Inch Height, 16 Inch Length, 0.20 In^2 Vent Area, Various G Levels	48
21.	Fluid Volume Vs. Fluid Height	52

LIST OF TABLES

TABLE		PAGE
I	Bond and Weber Numbers for Candidate Surface Tension Screens	7
II	Fuel Volume vs. Fuel Height for Nine-Inch Trap Tanks	30
III	Fuel Volume vs. Fuel Height for 3.2-Inch Trap Tank	32
IV	Trap Tank Volumes	44

SECTION I

INTRODUCTION

1. GENERAL CONSIDERATIONS FOR SELECTING SURFACE TENSION SCREENS

Fuel expulsion from the fuel tanks of ramjet-powered missiles has generally been accomplished by positive expulsion techniques, primarily elastromeric bladders or diaphragms pressurized by stored gas bottles or ram air. The missiles which have employed this technique have operated over moderate flight envelopes, primarily below Mach 3. In this flight envelope the aerodynamic heating and the ram air recovery temperatures were low enough to permit use of elastromeric bladders. Overall expulsion efficiencies achieved with these elastromeric systems were 95% or better. Although elastromeric expulsion techniques have proven useful in a number of ramjet-powered missiles their utility becomes less apparent for future systems operating at Mach numbers considerably above Mach 3. The thermal load imposed on the bladder above Mach 3 becomes so great that the structural integrity of the material becomes a problem. An obvious method of overcoming the thermal problem is to use a layer of insulation between the elastromeric material and the metal skin of the missile. This imposes a weight and volume penalty for a given missile configuration resulting in some decrease in performance of the missile.

Other expulsion techniques, shown in Figure 1, such as bellows, metallic bladders, pistons, and surface tension screens have been used for orientation and expulsion of fuel and oxidizers in a number of missile and space vehicle propulsion systems. All of these expulsion devices are driven by a pressurizing gas such as air or nitrogen (Reference 1). A cursory examination of these alternate expulsion techniques was performed for their application to the multipurpose missile (MPM). Although several of these expulsion techniques may be attractive, various factors such as pressure requirements and tank shape resulted in the selection of the surface tension screen concept for further in-house study.

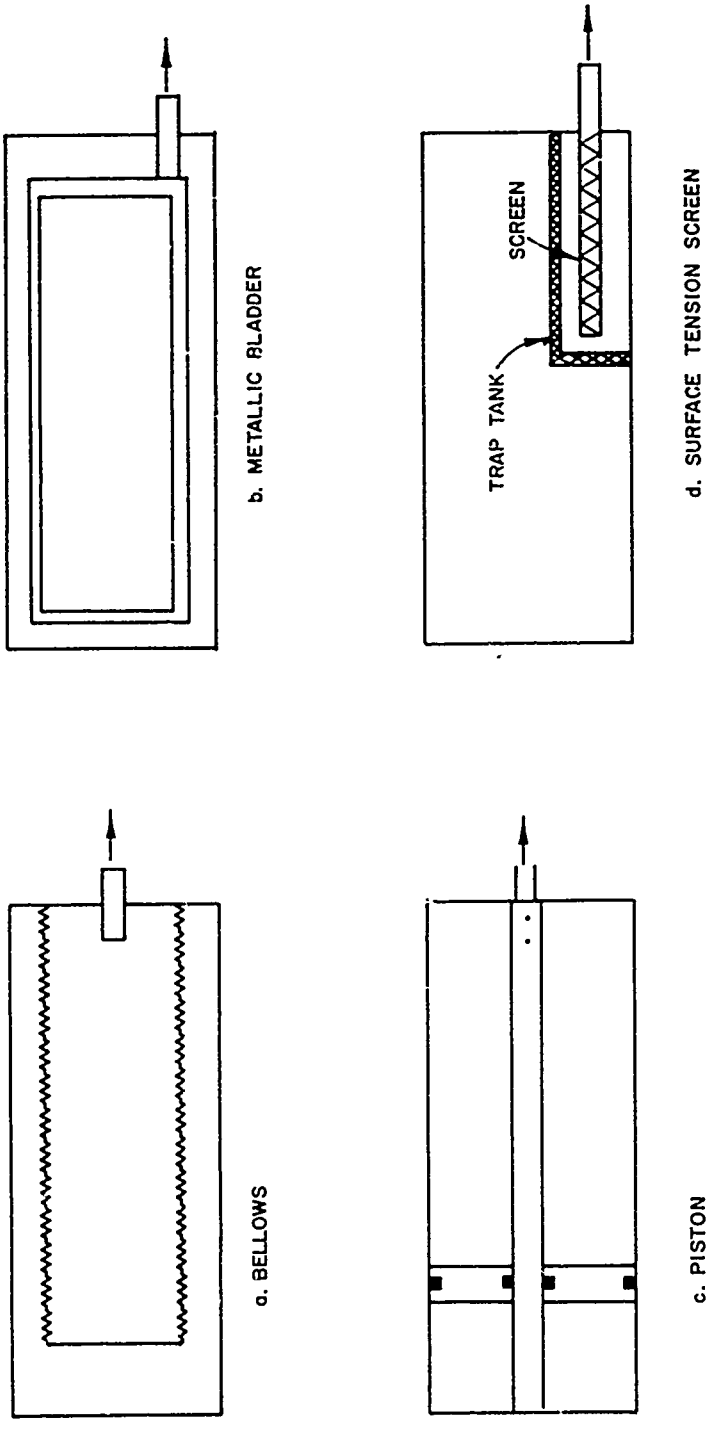

Figure 1. Candidate Expulsion Techniques

Figure 1d is a schematic of a typical surface tension screen system. One or more screens having hole sizes in the micronic range are contained inside a trap tank which holds fuel in contract with the screens during vehicle maneuvers which would otherwise rapidly uncover the surface tension screens. Fuel flows through the screen(s) by means of pressurizing the fuel tank with an inert gas such as nitrogen. The screen(s) permit only liquid to flow until the total pressure drop across the screen orifices exceeds the surface tension force of the liquid under consideration. (See Section II for operation principle). If this surface tension force is exceeded, gas ingestion in the screen(s) will occur and two-phase flow to the engine will result. The trap tank containing the surface tension screen(s) is perforated to allow fuel flow into the screen(s) and to permit the pressurizing gas to escape when the vehicle returns to normal "G" operation.

An analytical evaluation of the surface tension screen concept for application to future ramjet-powered missiles has been performed. Primary advantages of the surface tension screen over the bladder expulsion system are:

a. less inert weight and volume

b. no moving parts

c. no thermal limitation (same as total missile) for the device itself*

d. unlimited expulsion cycle capability (Reference 2).

2. DESIGN CONSIDERATIONS FOR SELECTION OF SURFACE TENSION SCREENS

The initial (and still primary) use of surface tension devices was for space vehicles under conditions of low or near zero gravity. The three primary forces which influence the dynamic behavior of liquid/gas systems are body forces, capillary forces, and viscous forces. The surface tension screen concept is effective only in systems where the capillary forces predominate. The relative importance of the body and

*Temperature will affect fluid properties which will affect efficiency of the surface tension device.

capillary forces for a specific case (i.e., evaluation of surface tension devices) can be estimated by three interrelated dimensionless parameters known as the Weber number, the Froude number, and the Bond number. The Weber number is defined as the ratio of inertial force to capillary force:

$$W_e = \frac{\rho V^2 d}{\sigma g_c} \tag{1}$$

where, W_e = Weber number, dimensionless

ρ = liquid density, lb-m/ft^3

V = liquid velocity through the surface tension screen, ft/sec

d = hole diameter of the surface tension screen, ft

σ = surface tension of the liquid, lb-f/ft

g_c = gravitational constant = $32.174 \frac{\text{lb-m ft}}{\text{lb-f sec}^2}$

For Weber numbers much greater than 1, capillary forces are insignificant so that liquid motion in the system is determined by the inertia of the system. For Weber numbers much less than 1, capillary forces dominate and define liquid movement in the system.

The Froude number provides an estimate of the inertia force to the gravitational force and is defined as follows:

$$F_r = \frac{V^2}{g_d} \tag{2}$$

where F_r = Froude Number, dimensionless

V = liquid velocity through the surface tension screen, ft/sec

g = local acceleration, ft/sec^2

d = hole diameter, ft

For Froude numbers very much greater than 1.0 the gravitational forces are sufficiently weak that they have essentially no influence on the

fluid motion whereas for very small values of the Froude number the gravitational forces must be considered.

The Bond number is the ratio of the gravitational forces to the capillary forces and is obtained by dividing the Weber number by the Froude number.

$$B_o = \frac{W_e}{F_r} = \frac{\frac{\rho V^2 d}{\sigma g_c}}{\frac{V^2}{gd}} = \frac{\rho g d^2}{\sigma g_c} \qquad (3)$$

For very small values of the Bond number, the capillary forces predominate in determing liquid motion whereas the gravitational force predominates for large Bond numbers. Figure 2 depicts the three hydrodynamic regimes defined by the Froude, Weber, and Bond numbers. A number of calculations were performed to evaluate the hydrodynamic regime anticipated for the surface tension screens considered by this analysis. These calculations were performed for a single screen element. The screen considered was one currently available from the Western Filter Company and was evaluated by Vought Missile and Space Company (VMSC) for use in the Harpoon missile. The total screen area for this particular element is 160 in^2 (1.11 ft^2) with a porosity of 30.7%. The fuel flow area therefore is 0.3411 ft^2. The screen tested by VMSC was a 10 micron unit. For this analysis, 44 and 100 micron screen sizes were assumed in addition to the 10 micron baseline screen. Flow area was kept constant at 0.3411 ft^2 for the larger hole sizes. Bond numbers and Weber numbers were calculated for the three hole sizes for fuel flow rates of 1.0 and 10 pounds per second and for acceleration forces of 1.0 and 10 g's. Results are presented in Table I.

The Bond numbers obtained ranged from 2.64×10^{-5} up to 2.45×10^{-2}. Weber numbers obtained ranged from 2.77×10^{-5} up to 4.85×10^{-2}. Referring to Figure 2, it is seen that these low values of the Bond and Weber numbers place the flow through these surface tension screens in the capillary-dominated regime. The primary reason for these low

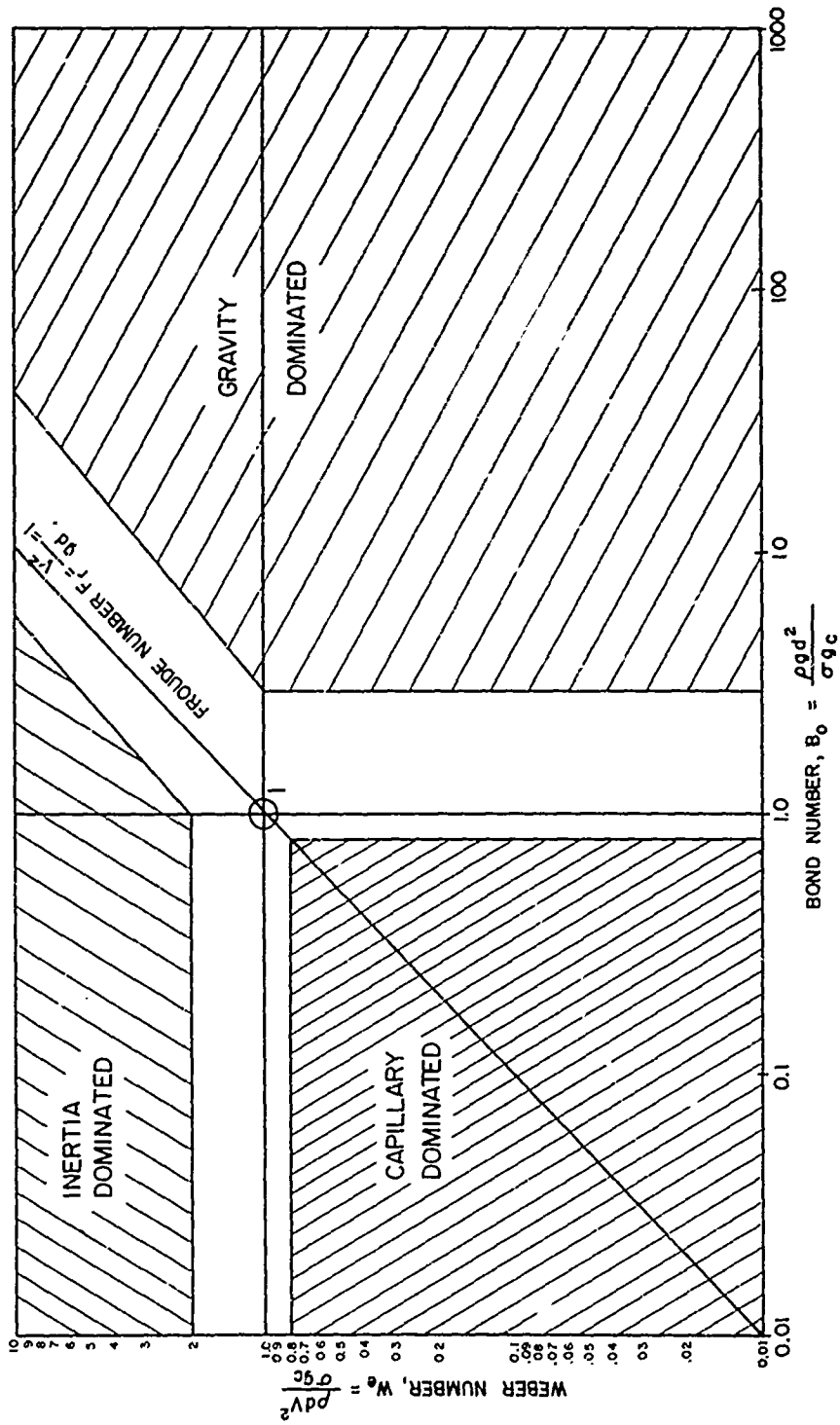

Figure 2. Hydrodynamic Regimes

TABLE I. BOND AND WEBER NUMBERS FOR CANDIDATE SURFACE TENSION SCREENS

HOLE SIZE, MICRONS	HOLE DIAMETER, FEET x 10^{-4}	FUEL TEMP. °F	WEBER NUMBER, DIMENSIONLESS	FUEL DENSITY, $\frac{LB\text{-}M}{FT^3}$	FUEL SURFACE TENSION $\frac{LB\text{-}F}{FT} \times 10^{-4}$	$\frac{g}{gc}$, $\frac{lb\text{-}f}{lb\text{-}m}$	FUEL FLOW, $\frac{LB\text{-}M}{SEC}$	FUEL VELOCITY, $\frac{FT}{SEC}$	BOND NUMBER, DIMENSIONLESS
100	3.28	77	4.85×10^{-4}	66.62	27.16	1	1	0.0440	2.64×10^{-3}
100	3.28	77	4.85×10^{-2}	66.62	27.16	1	10	0.4401	2.64×10^{-3}
100	3.28	77	4.85×10^{-2}	66.62	27.16	10	1	0.0440	2.64×10^{-2}
100	3.28	77	4.85×10^{-2}	66.62	27.16	10	10	0.4401	2.64×10^{-2}
44	1.44	77	2.13×10^{-4}	66.62	27.16	1	1	0.0440	5.09×10^{-4}
44	1.44	77	2.13×10^{-2}	66.62	27.16	1	10	0.4401	5.09×10^{-4}
44	1.44	77	2.13×10^{-4}	66.62	27.16	10	1	0.0440	5.09×10^{-3}
44	1.44	77	2.13×10^{-2}	66.62	27.16	10	10	0.4401	5.09×10^{-3}
10	0.328	77	4.85×10^{-5}	66.62	27.16	1	1	0.0440	2.64×10^{-5}
100	3.28	0	4.50×10^{-4}	68.44	30.06	1	1	0.0440	2.45×10^{-3}
100	3.28	0	4.50×10^{-2}	68.44	30.06	10	10	0.4401	2.45×10^{-2}
10	0.328	0	$2.77 \times 10^{-}$	68.44	30.06	1	1	0.0440	2.45×10^{-5}
10	0.328	0	4.50×10^{-3}	68.44	30.06	10	10	0.4401	2.45×10^{-4}

values of the Bond and Weber numbers in the surface tension screens is the extremely small hole diameters considered. This is seen by examining Equation 1 for the Weber number where the hole diameter is to the first power in the numerator and by examining Equation 3 for the Bond number where the hole diameter is to the second power in the numerator. Also contributing to the low Weber numbers is the fact that the velocity through the screens is less than 1 ft/sec. Since the velocity is to the second power in the numerator, the velocity term becomes extremely important in producing small Weber numbers as the velocity through the screen is decreased below 1 ft/sec.

The other factors used to define these dimensionless parameters (Bond and Weber numbers) are less important than the screen dimensions. This can be seen by examining the results presented in Table I. Reducing the fuel temperature from 77°F to 0°F produces only minor changes in the Bond and Weber numbers as does increasing acceleration level from 1 g to 10 g's. Thus, one could conclude that these screens should perform well with RJ-5 fuel since the Bond and Weber numbers indicate that the flow is in the capillary-dominated regime. However, one extremely important fuel property not included in the Bond and Weber numbers is viscosity. As will be shown later, this property is critical to the performance of surface tension screens.

SECTION II

PRIMARY DESIGN PARAMETERS

1. PRINCIPAL OF OPERATION

The operation of surface tension screens utilizes capillary force as the governing parameter. The technique generally used to expell fuel from fuel tanks containing surface tension screens is to pressurize the tank with an inert gas to a sufficiently high pressure to maintain the fuel flow rate required by the engine. Near the end of a flight when the fuel supply is low or during certain maneuvers of the missile which produce negative G operation, the surface tension screen(s) may be exposed to the pressurizing gas. Since two phase flow to the engine cannot be tolerated, the fuel expulsion system must be designed to prevent gas ingestion. The operation of a surface tension screen is shown schematically in Figure 3. The situation depicted in Figure 3 is for a positive g low fuel level condition which results in partial exposure of the surface tension screen. The principle of operation, however, is not altered for negative g orientation of the fuel tank.

The basic condition which must be met to permit gas-free liquid to flow is that the total pressure differential between the gas and liquid at all points across the screen must be less than the surface tension pressure force. This inequality can be expressed as follows:

$$\Delta P_T < P\sigma \tag{4}$$

where ΔP_T = total pressure differential across surface tension screen orifice, lb-f/ft^2

$\Delta P\sigma$ = surface tension pressure drop across screen orifice, $\frac{\text{lb-f}}{\text{ft}^2}$

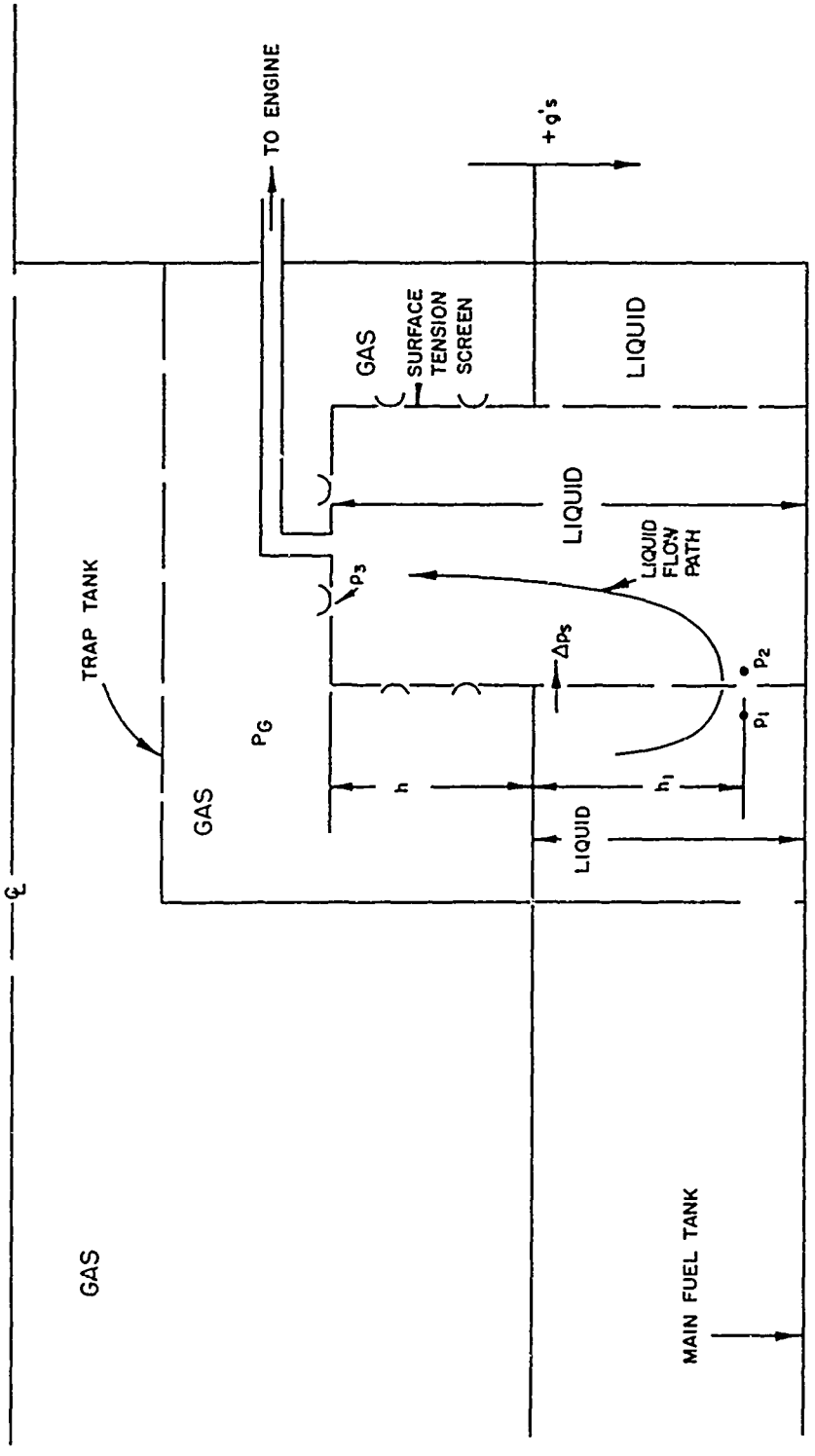

Figure 3. Operation Principle of Surface Tension Screens

From Figure 3, it is seen that the total pressure differential across a surface tension screen orifice, ΔP_T, is given by the difference in the gas pressure outside the screen minus the total pressure inside the screen. Expressed mathematically, this pressure differential is as follows:

$$\Delta P_T = P_G - P_{Ti} \tag{5}$$

where P_{Ti} is the total internal pressure.

If the gas pressure, P_G, is constant then the pressure differential across the screen is maximum at the point of minimum pressure within the surface tension screen. From Figure 3, this minimum point is seen to occur at the outlet plane, P_3, since the maximum flow and head losses have occurred at that point. Therefore, Equation (5) becomes:

$$\Delta P_{T_{MAX}} = P_G - P_3 \tag{6}$$

Equation 6 holds as long as two phase flow does not occur.

The pressure at P_3 is equal to the gas pressure, P_G, minus the pressure losses which occur along the liquid flow path (See Figure 3). These pressure losses are determined as follows:

$$P_1 = P_G + P_{h_1} \tag{7}$$

where P_1 = total pressure at any given point in trap tank outside surface tension screen, lb-f/ft^2

P_G = pressurant gas pressure, lb-f/ft^2

P_{h_1} = pressure of liquid head at any given point in trap tank outside of surface tension screen, lb-f/ft^2

The pressure at the same liquid level inside the surface tension screen is:

$$P_2 = P_1 - \Delta P_s \tag{8}$$

$$P_2 = P_G + P_{h_1} - \Delta P_s \tag{9}$$

where ΔP_s is liquid pressure drop across the surface tension screen orifice, lb-f/ft^2.

The pressure at the screen outlet plane, P_3, is

$$P_3 = P_2 - P_{h_1} - P_h - \Delta P_F \tag{10}$$

or

$$P_3 = P_G + P_{h_1} - \Delta P_s - P_{h_1} - P_h - \Delta P_F$$

which simplifies to:

$$P_3 = P_G - P_h - \Delta P_s - \Delta P_F \tag{11}$$

where P_h = pressure of liquid head inside screen above trap tank level, $\frac{\text{lb-f}}{\text{ft}^2}$

ΔP_F = flow friction loss, lb-f/ft^2

Therefore, from Equation 6, the largest pressure differential across the portion of the surface tension screen exposed to gas is:

$$\Delta P_{T_{MAX}} = P_G - (P_G - P_h - \Delta P_s - \Delta P_F) \tag{12}$$

which reduces to

$$\Delta P_{T_{MAX}} = P_h + \Delta P_s + \Delta P_F \tag{13}$$

As the fuel level in the trap tank decreases, each of the terms in Equation 13 increases, assuming positive g operation and a constant flow rate out of the surface tension screen. That this is true can be seen by the following reasoning:

a. Liquid height used to obtain head pressure (P_h) increases as trap tank level decreases resulting in higher head pressure.

b. For a constant flow rate, the screen flow pressure drop increases with decreasing trap tank liquid level since the flow area decreases with decreasing liquid level of the trap tank.

c. Flow friction pressure drop increases with decreasing trap tank liquid height since the percentage of fuel which must travel the longer distance to the outlet is increased.

The surface tension pressure, ΔP_σ, can be calculated for a given surface tension screen by the following equation (Reference 3):

$$\Delta P_\sigma = \frac{4\sigma}{d} \tag{14}$$

where σ = surface tension of liquid, lb-f/ft^2

d = hole diameter of surface tension screen, ft

This pressure drop can be expressed in terms of liquid head by utilizing the following relationship:

$$\Delta P\sigma = h_\sigma \frac{g\rho}{g_c} \tag{15}$$

where ρ = density of liquid, $\frac{\text{lb-m}}{\text{ft}^3}$

h_σ = height of liquid, ft

g = local acceleration, ft/sec^2

g_c = gravitational constant, 32.174 $\frac{\text{lb-m ft}}{\text{lb-f sec}^2}$

Rearranging Equation 15 gives,

$$h_\sigma = \frac{\Delta P \sigma}{\rho \frac{g}{g_c}} \tag{16}$$

Substituting Equation 14 into 16 produces:

$$h_\sigma = \frac{4\sigma}{d \frac{g}{g_c} \rho} \tag{17}$$

Equation 17 gives the maximum pressure in terms of liquid head which a surface tension screen can support as a function of liquid properties (surface tension and density), hole size, and acceleration (g) level, before gas flow will occur across the screen. Figure 4 shows the retention capability of various screen sizes as a function of temperature and imposed acceleration levels for RJ-5 fuel. From Equation 17 it is seen that retention capability is inversely proportional to hole diameter and to acceleration (g) level. For example, from Figure 4, the liquid head for RJ-5 with the 10 micron size screen under a 1 g load is rapidly decreased to a low value by increasing the hole diameter or by increasing the g loading. Temperature of the fuel has a less drastic effect since the decrease in retention capability from -65°F to +500°F is only about 50% of the -65°F value.

Equation 4 is the basic inequality which must exist for surface tension screen operation. This inequality can be expressed in terms of liquid head by converting the pressure drop terms to liquid head terms. The resulting expression is:

$$h_h + h_s + h_F < h_\sigma \tag{18}$$

where h_h = liquid head inside screen above trap tank level, ft

h_s = equivalent liquid head due to flow through screen, ft

h_F = equivalent liquid head due to flow friction losses inside due to surface tension of the fluid, ft

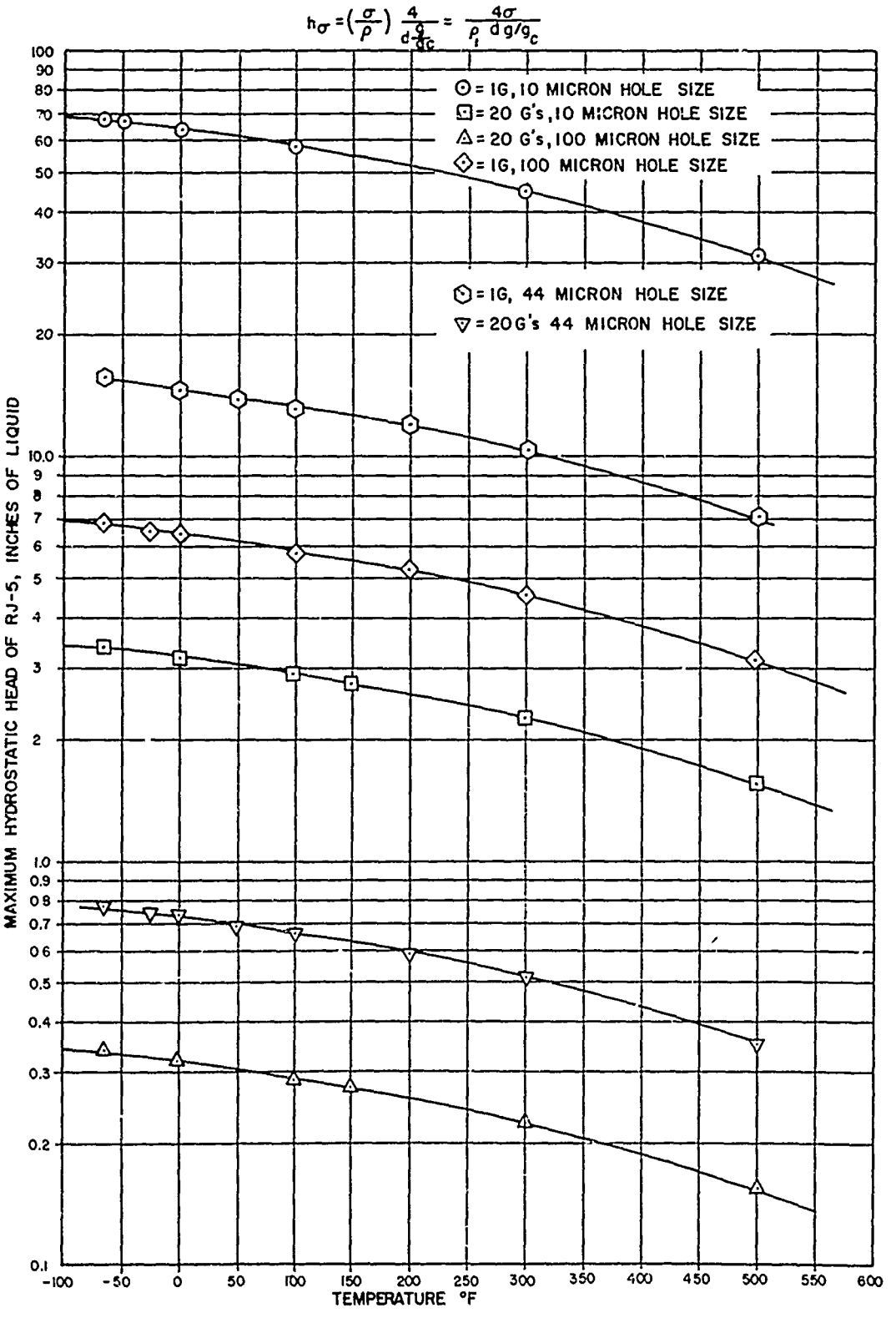

Figure 4. Retention Capability of Surface Tension Screens

Thus, it is seen that in the operation of a surface tension screen the total liquid head due to height and flow losses must be less than the maximum liquid head which a screen can support based on the surface tension of the liquid.

The most difficult factor to evaluate is the equivalent head due to pressure drop across the screen, h_s. A number of papers (References 4, 5, and 6) have been published giving correlations for obtaining screen pressure drops. Assumptions used in these correlations have included the following models for flow through the screen:

(1) Orifices or Nozzles in Parallel (Reference 4)

The flow through a screen can be considered as flow through a number of orifices or nozzles in parallel. Thus, the pressure drop or head loss across a screen can be computed from an orifice-type equation. The resulting equation for head loss is:

$$h_s = \frac{n}{C^2}\left(\frac{1-\alpha^2}{\alpha^2}\right)\frac{V^2}{2g} \tag{19}$$

where h_s = head loss across screen, feet of fluid flowing

n = number of screens in series, dimensionless

C = screen discharge coefficient, dimensionless

α = fractional free projected area of screen, dimensionless

V = superficial velocity ahead of screen, ft/sec*

g_c = gravitational acceleration, 32.17 ft/sec^2

Experimental data [Volokhov, Vestnik, Ing. Techn., (Reference 4), 149-152 (1930)] indicate that for a series of screens the overall head loss is directly proportional to the number of screens in series, as given by Equation 19, and is not affected by either the spacing between successive screens or by their orientation with respect to one another.

---

*$V = \frac{Q}{A}$ where Q = volumetric flow rate, $\frac{ft^3}{sec}$ and A = flow area, ft^2.

Screen discharge coefficient "C" is a function of screen Reynolds number,

$$N_{Re} = \frac{D_S V \rho}{\alpha \mu} \tag{20}$$

where D_S = aperture width, ft

ρ = fluid density, lb-m/ft^3

μ = fluid viscosity, lb-f/(ft)(sec)

For plain rectangular-mesh screens, Lapple's plot of C vs N_{Re} is given in Figure 5. This curve represents most of the data to within 20 percent. Coefficients greater than 1 probably indicate that the effective free area is larger than that of the projected area and that there is partial recovery of head due to the downstream rounding of the wires.

(2) Packed Bed (Reference 5)

This model was developed for flow of Newtonian fluids through all types of woven metal screens. The screen is treated as a very thin packed bed in which the pressure drop across the screen is considered to be the sum of both viscous and inertial forces. The model correlates friction factor versus Reynolds Number. Pressure drop is included in the friction factor term so that once the friction factor is obtained from a plot of Reynolds Number vs friction factor, the pressure drop through the screen can be calculated. The model was developed by using experimental data of pressure drop vs. velocity for nitrogen over a velocity range from 0.1 to 30 ft/sec. This correlation was shown to hold for Reynolds Numbers up to 1000 for water as the test fluid by substituting data obtained by an earlier investigator into the correlation equation. Results obtained were within the experimental error of the nitrogen data.

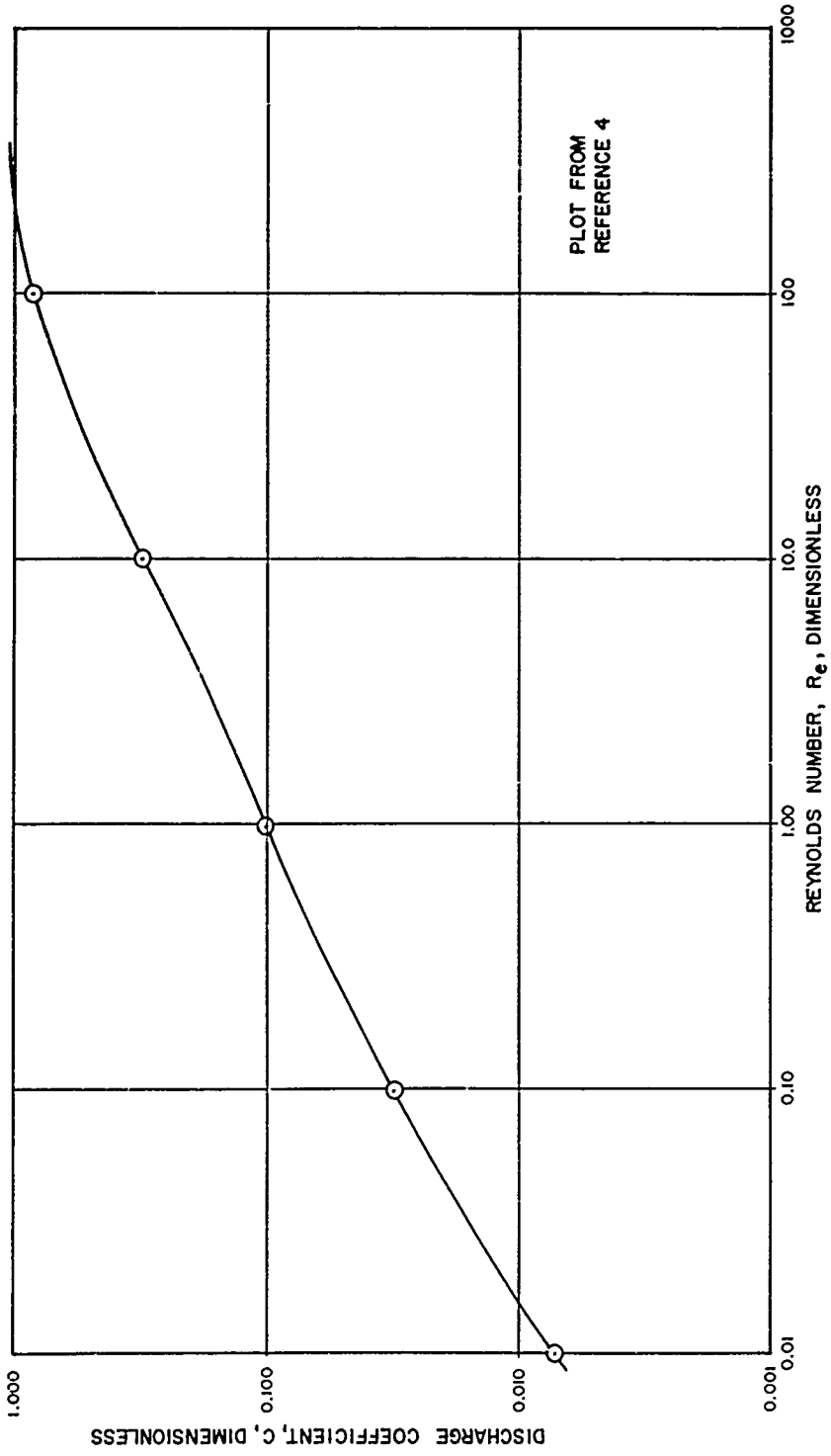

Figure 5. Screen Discharge Coefficients for Surface Tension Screens

(3). Win Tec Pressure Drop Model

The model currently being used by McDonnell Douglas Astronautics Company for their surface tension screen work on the Harpoon missile was developed by the Win Tec Corporation under a NASA contract (Reference 7). This model correlated screen pressure drop data for JP-4, water, hydrazine, ethylene glycol/water mixtures, liquid nitrogen, and hydraulic oil much better than the original model (Reference 8) used by McDonnell Douglas.

(4). Other Methods

Other methods of correlating overall frictional losses across screens are given by Cornell [Trans. Am. Soc. Mech. Engrs., 80, 791-799 (1958)] and Grootenhuis [Proc. Inst. Mech. Engrs. 168A, 837-846 (1954)].

2. SCREEN PRESSURE DROP CALCULATIONS

Pressure drop through surface tension screens as a function of mass flow rate were calculated for RJ-5 at three fuel temperatures using the Reference 4 technique described in subparagraph 1 above*. Two screen sizes (44 and 100 microns) were used and all calculations were for the one g level. Results are shown in Figure 6. The following example will demonstrate the impact of the Figure 6 data:

EXAMPLE 1: Use 44 micron screen at 1 g

Fuel Temperature = 77°F

From Figure 4, $h_{\sigma'}$ = 13.3 inches of RJ-5

Equation 18 then becomes: $13.3 > h_h + h_s + h_F$ or $13.1 - h_s > h_h + h_F$. h_s is obtained from Figure 6 assuming maximum flow rate of 10 lb/sec. h_s = 1.05 ft of RJ-5 = 12.6 inches of RJ-5. Then, $13.3 - 12.6 > h_h + h_F$. Thus, the total allowable pressure drop for the head and the channel

*The Reference 4 technique is used since the accuracy required in this analysis did not warrant use of the more complex technique.

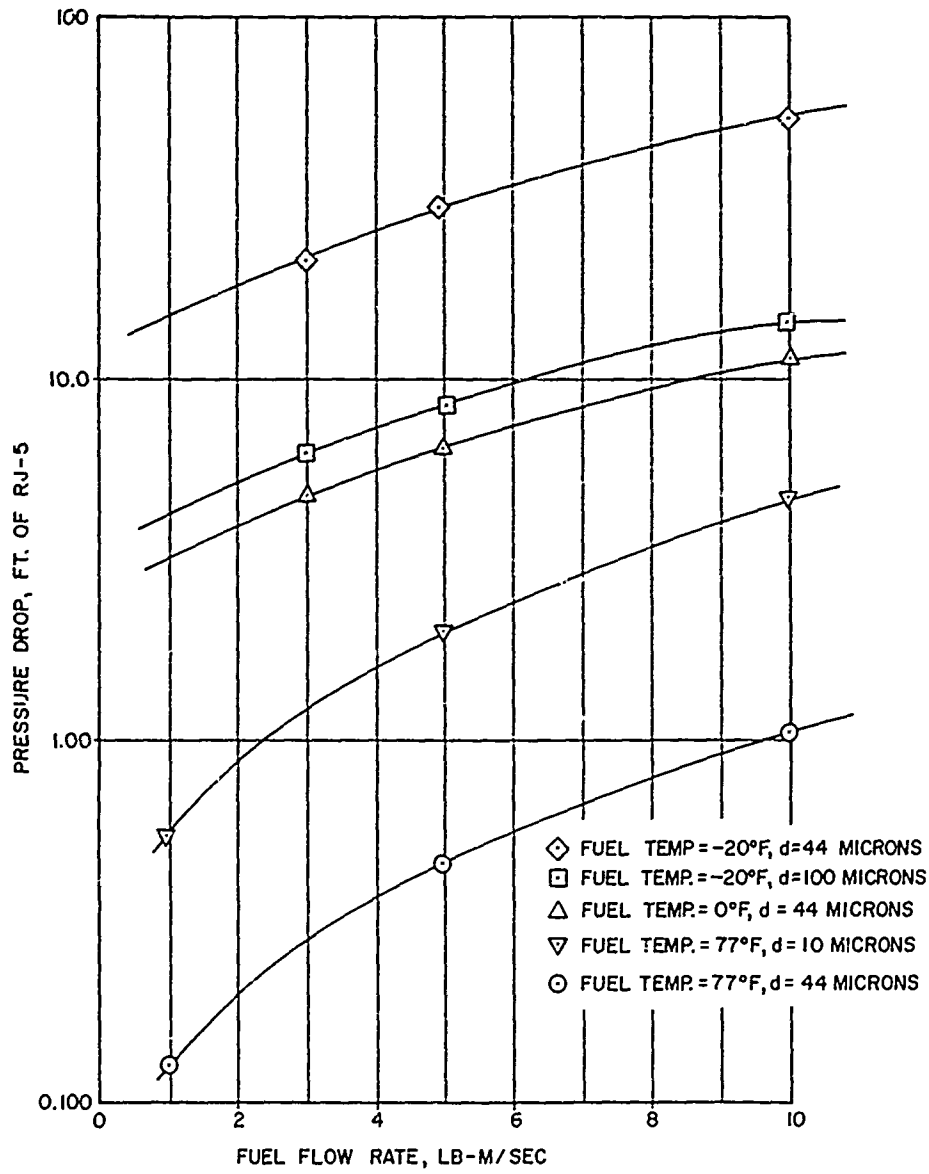

Figure 6. Surface Tension Screens Pressure Drops

flow pressure drops is only 0.7 of an inch of RJ-5. Thus, even if the channel flow pressure drop is ignored (a reasonable assumption) the total liquid head which the surface tension screen can withstand is only 0.7 of an inch of RJ-5.

Using the same conditions as Example 1 except for fuel temperature = 0°F, it is seen that the maximum allowable pressure drop is exceeded:

From Figure 4, h_σ = 14.5 inches of RJ-5

From Figure 6, h_s = 11.5 ft of RJ-5

= 138 inches of RJ-5

Then, from Equation 18, $h_h + 138 + h_F < 14.5$.

Thus, the allowable pressure drop of 14.5 inches of RJ-5 is overwhelmed by the 138 inches of pressure drop through the screen. This means, of course, that if the system were pressurized to overcome this screen pressure drop, ingestion of the pressurant gas would occur.

Even though the pressure drop through the screen decreases with fuel flow rate, the screen pressure drop still exceeds the allowable limit for the 44 micron screen with 0°F fuel for the entire range of fuel flow rates of interest.

The primary reason for the excessive pressure drop through the screen is the high viscosity of the RJ-5 fuel. This can be seen by examining Equation 18 which shows that the head loss through the screen is inversely proportional to the square of the screen discharge coefficient. As shown by Figure 5, the screen discharge coefficient is a function of the Reynolds Number of the fuel in the screen. Because Reynolds Number is inversely proportional to the fuel viscosity (see Equation 19) large values of viscosity produce small Reynolds Numbers. From Figure 5, it is seen that small values of the Reynolds Number correspond to small values of the screen discharge coefficient which, in turn, produce large pressure drops when inserted into Equation 18. For this study, Reynolds

Numbers through the screens of less than 1.0 were generally obtained. These low values of the Reynolds Number correspond to screen discharge coefficient much less than 0.1 which when inserted into Equation 18 produced high values of the screen pressure drop.

The technique used by McDonnell Douglas to calculate pressure drop across surface tension screens demonstrates the effect of viscosity more directly. The current correlation used by McDonnell Douglas was developed by the Win Tec Corporation under a NASA contract (Reference 7). The correlation is:

$$\Delta P_s = a\rho Q^2 + b\mu Q \qquad (21)$$

where, ΔP_s = screen pressure drop, lb/in^2

a,b = constants for specific screen size and type

ρ = liquid density, gm/ml

μ = liquid viscosity, centipoise

Q = volumetric flow rate per unit area, $\frac{\text{gallons per minute}}{in^2}$

Using Equation 21 for the two pressure drop calculation examples previously given produces the results shown below:

EXAMPLE 1: 44 micron screen at 1 g with fuel temperature of 77°F

Constants a and b are obtained from Reference 8.

$a = 0.027$

$b = 0.070$

$$Q = \frac{10\ \text{lb-m}}{\text{sec}} \times \frac{1}{9.0\ \frac{\text{lb-m}}{\text{gallon}}} \times 60\ \frac{\text{sec}}{\text{min}} \times \frac{1}{160\ in^2}$$

$$Q = \frac{600\ \text{gallons}}{1400\ \text{min sec}^2} = 0.4167\ \frac{\text{gallons}}{\text{min in}^2}$$

$\rho = 1.07$ gm/ml

$\mu = 24.8$ centipoise

$$\Delta P_s = 0.027 \times 1.07 \times (0.4167)^2 + 0.070 \times 24.8 \times 0.4167$$

$$\Delta P_s = 0.00502 + 0.72339$$

$$\Delta P_s = 0.72841 \text{ lb/in}^2$$

This pressure can be converted to inches of liquid as follows:

$$h_s = \frac{P_s}{\rho g} = \frac{0.72841 \text{ lb/in}^2}{0.03856 \frac{\text{lb}}{\text{in}^3} \times 1}$$

$$h_s = 18.89 \text{ inches}$$

EXAMPLE 2: Fuel Temperature = 0°F

Therefore, $\rho = 1.101$ gm/ml

$\mu = 231$ centipoise

$$\Delta P_s = 0.027 \times 1.101 \times (0.4167)^2 + 0.070 \times 231 \times 0.4167$$

$$\Delta P_s = 0.00516 + 6.73804$$

$$\Delta P_s = 6.7432 \text{ lb/in}^2$$

Converting to liquid head,

$$h_s = \frac{6.7432}{0.03978 \times 1} = 169.5 \text{ inches}$$

These two examples demonstrate the effect of viscosity on screen pressure drop. Decreasing the temperature from 77°F to 0°F increased the screen pressure drop by nearly an order of magnitude. Even at 77°F the screen pressure drop obtained by this technique exceeds the total permissible pressure drop (13.3 inches) for this surface tension screen. (See original Example 1 calculation). The effect of the other parameters in Equation 20 on screen pressure drop is much less drastic than viscosity. The constants a and b will vary with specific screen type but will vary only by a factor of about two for the constant a and about four for the constant b for the screens used in this study. Viscosity varies by a factor of about nine between 77°F and 0°F and of course becomes much

greater as the fuel temperature is decreased toward -65°F. The variance of density is negligible compared to the variance in the other parameters. The final parameter is volumetric flow rate per unit area. This parameter will be less than one unless a fairly small screen is used. Therefore, this parameter has much less effect on screen pressure drop than does viscosity since it is squared in the first term of Equation 21 and is multiplied by viscosity in the second term of Equation 21. Thus, it is seen that viscosity is the primary parameter controlling pressure drop across surface tension screens when one is considering a high viscosity fluid such as RJ-5.

SECTION III

TRAP TANK SIZING

1. TRAP TANK GEOMETRY AND CALCULATION PROCEDURES

During normal positive acceleration flight conditions the trap tank containing the surface tension screens is completely covered and filled with fuel so that fuel movement (sloshing) in the main tank has minimal effect on the operation of the surface tension units. During certain maneuvers of the missile, however, negative g conditions will exist which will uncover the trap tank for short periods of time. The essential requirement for the trap tank is to supply sufficient fuel for the length of time of the negative g maneuver so that the engine will not flame out. An analysis of the retention time provided by trap tanks for use in the Harpoon missile is presented in Reference 3. This analytical technique has been adapted for use with RJ-5 and is presented in the following paragraphs.

The trap tank flow model used for the retention time analysis is shown in Figure 7. The total volumetric fuel flow rate out of the tank is given by

$$\frac{dv}{dt} = \frac{\dot{m}}{\rho} + A\sqrt{2g\ hG} \tag{22}$$

where $\frac{dv}{dt}$ = total volumetric flow rate, ft^3/sec

$\dot{m}$ = engine mass flow rate, lb-m/sec

ρ = fuel density, $lb\text{-}m/ft^3$

A = total effective orifice area, ft^2

g = gravitational acceleration, 32.17 ft/sec^2

h = fluid height above orifice, ft

G = number of negative G's, dimensionless

Assuming that the fluid volume is linear with fluid height gives,

$$V = a + kh \tag{23}$$

where a and k are constants. Differentiating Equation 23 and noting that fluid height decreases with time gives

$$\frac{dv}{dt} = -k\,\frac{dh}{dt} \tag{24}$$

Equating Equations 22 and 24 gives

$$-k\,\frac{dh}{dt} = \frac{\dot{m}}{\rho} + A\sqrt{2g\,hG} \tag{25}$$

Integration of Equation 25 and insertion of the boundary conditions of $h = h_o$ at $t = 0$ gives the following expression relating fluid height with time:

$$t = \frac{2k}{\alpha^2}\left[\alpha(h_o^{1/2} - h^{1/2}) + Q_e \ln\left(\frac{Q_e + \alpha h^{1/2}}{Q_e + \alpha h_o^{1/2}}\right)\right] \tag{26}$$

where $\alpha = A\sqrt{2gG}$

$Q_e = \frac{\dot{m}}{\rho}$

The initial calculation made was for the volume of fuel left in the trap tank as a function of fuel height. The configuration of the trap tank considered for this analysis is shown in Figures 7 and 8. From the schematic shown in Figure 8, the following geometrical relationships are derived:

$$\cos\theta = \frac{R-H}{R} \tag{27}$$

$$\sin\theta = \frac{C/2}{R} = \frac{C}{2R} \tag{28}$$

$$S = 2R\,\theta \tag{29}$$

$$H = R(1-\cos\theta) \tag{30}$$

$$C = 2R\sin\theta \tag{31}$$

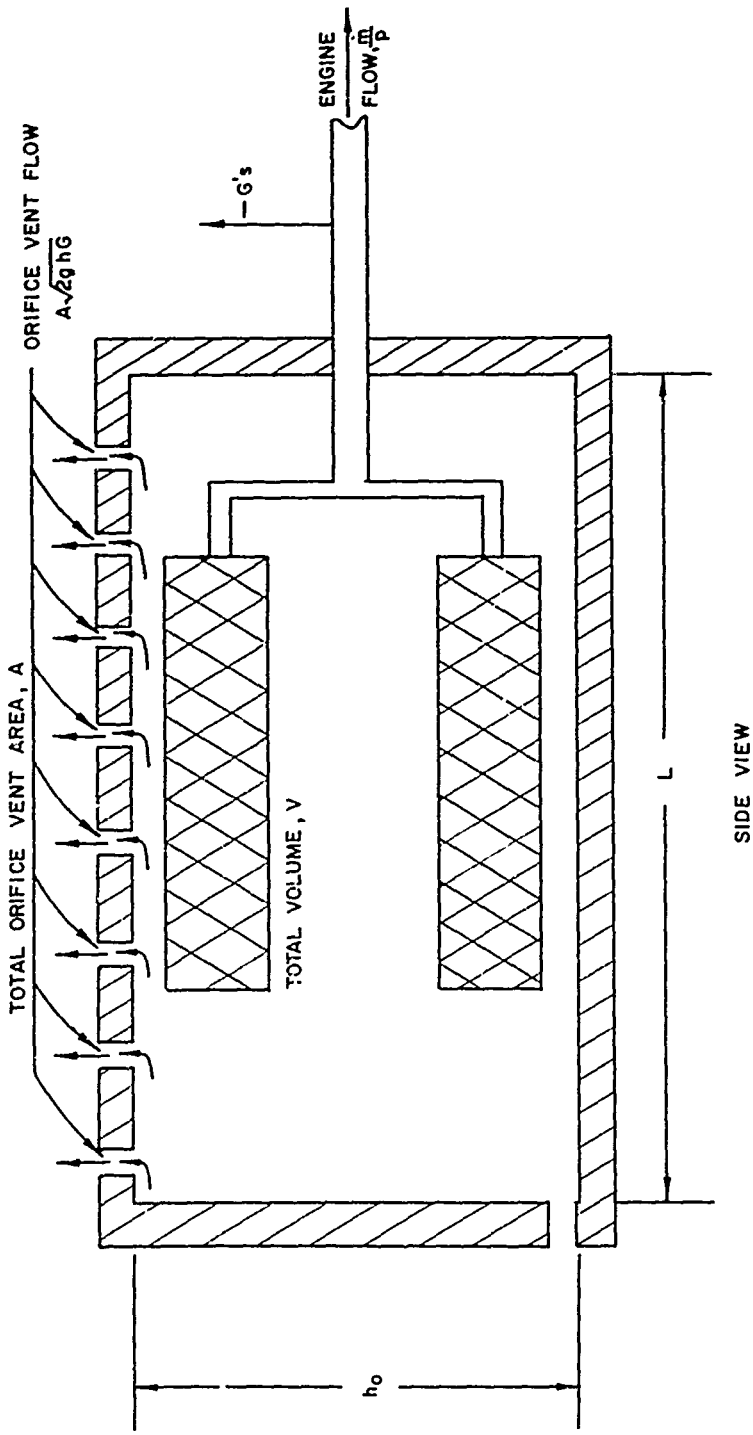

Figure 7. Trap Tank Flow Model

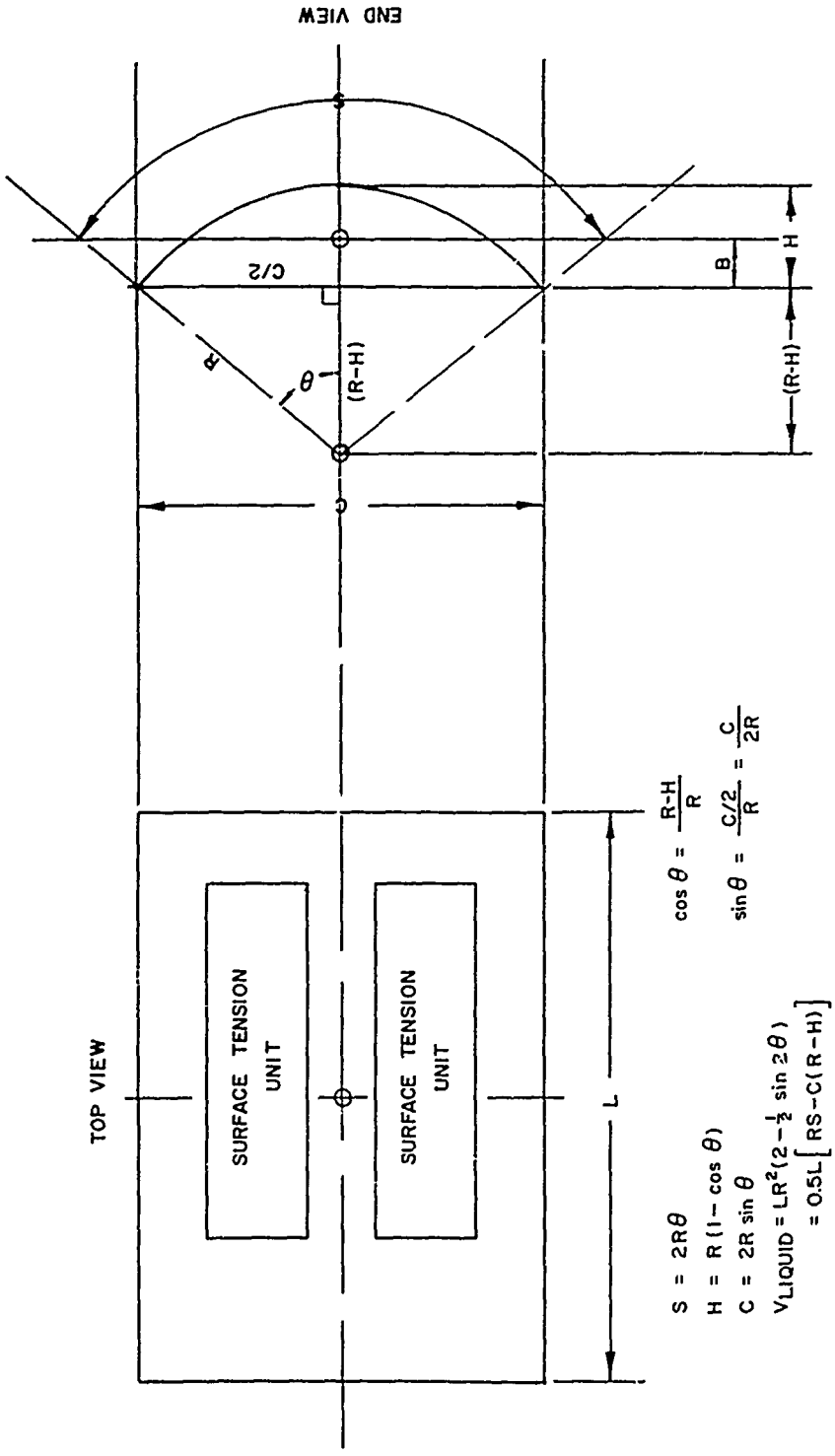

Figure 8. Trap Tank Schematic

where,

R = Radius of main tank, inches

H = height of liquid in trap tank, inches

C = width of liquid in trap tank, inches

θ = half-angle formed by radii drawn from main tank center to the intersection of liquid level with trap tank wall, radians

The volume of liquid is given by the following equation:

$$V_{LIQUID} = LR^2(\theta - 1/2 \text{ Sin } 2\theta)$$

$$\text{or } V_{LIQUID} = \frac{L}{2}[RS-C(R-H)] \qquad (32)$$

L = Trap tank length, inches

Variation of fuel volume as a function of fuel height was obtained for two trap tank heights. The first trap tank considered was a 9-inch trap tank height with the main fuel tank being 18 inches in diameter. Trap tank lengths of 6, 9, and 12 inches were used to obtain three trap tank sizes. Results of the calculations for the first trap tank height are presented in Table II and shown graphically by Figure 9. The data points plotted in Figure 9 are solutions to Equation 32. These data are then approximated by two linear segments for each tank size so that slopes and the point where the slopes change could be obtained for each tank size. The linear approximation provides the constant required in Equation 23. As will be shown later, this information is necessary for obtaining fuel expulsion times from the trap tanks.

The second trap tank considered had a height of 3.2 inches with a length of 16 inches. The main tank diameter was maintained at 18 inches. Table III presents the fuel volume as a function of fuel height for this tank. Figure 10 shows the trap tank fuel volume as a function of fuel height. Again, the data obtained was plotted as two linear segments so that fuel expulsion times could be obtained.

TABLE II - FUEL VOLUME VS. FUEL HEIGHT FOR NINE-INCH TRAP TANKS

TANK 1 - 6 INCH LENGTH		TANK 2 - 9 INCH LENGTH		TANK 3 - 12 INCH LENGTH	
Fuel Height, In	Volume, In^3	Fuel Height, In.	Volume, In^3	Fuel Height, In	Volume, In^3
9.0	763.4	9.0	1145.1	9.0	1526.8
7.5	599.7	8.0	983.4	8.0	1311.3
6.0	445.6	7.0	823.8	7.0	1098.4
4.5	298.5	6.0	668.3	6.0	891.0
3.5	208.5	5.0	519.1	5.0	692.2
3.0	167.2	4.0	379.0	4.0	505.3
2.0	92.8	3.25	281.6	3.5	417.6
1.5	60.7	3.0	250.9	3.0	334.5
1.0	33.4	2.5	192.6	2.5	256.9
		2.0	139.1	2.0	185.5
		1.5	91.2	1.5	121.5
		1.0	50.1	1.0	66.7
		0.5	17.9	0.5	23.8

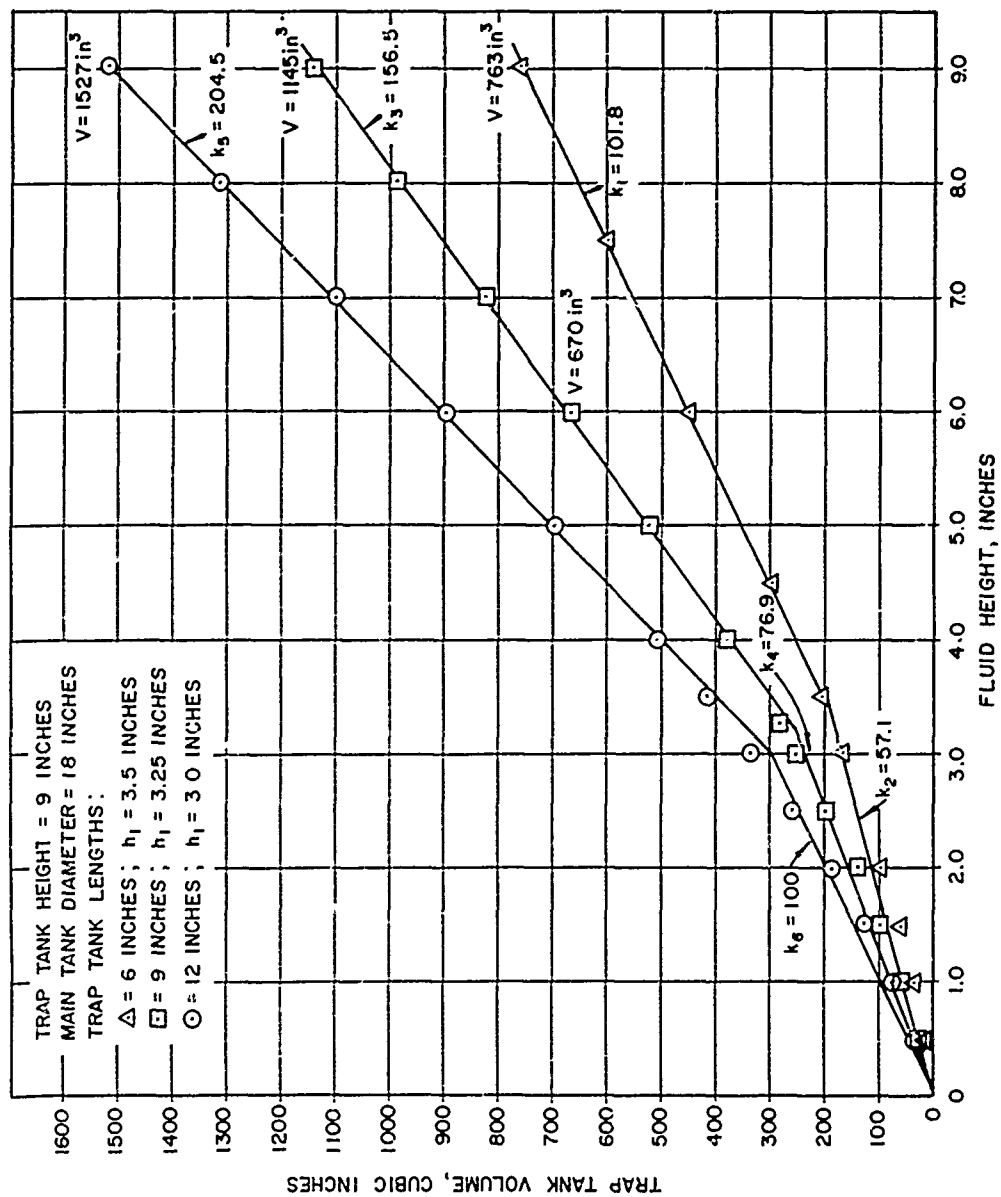

Figure 9. Trap Tank Fuel Volume Versus Fuel Height for 9 Inch Tank

TABLE III - FUEL VOLUME VS. FUEL HEIGHT FOR

3.2 INCH HIGH TRAP TANK

FUEL HEIGHT, INCHES	FUEL VOLUME, $INCHES^3$
3.2	489.5
3.0	446.0
2.6	362.6
2.2	284.3
2.0	247.3
1.8	211.9
1.6	178.2
1.4	146.4
1.2	116.6
1.0	89.0
0.9	76.1
0.8	63.9
0.6	41.6
0.4	22.7

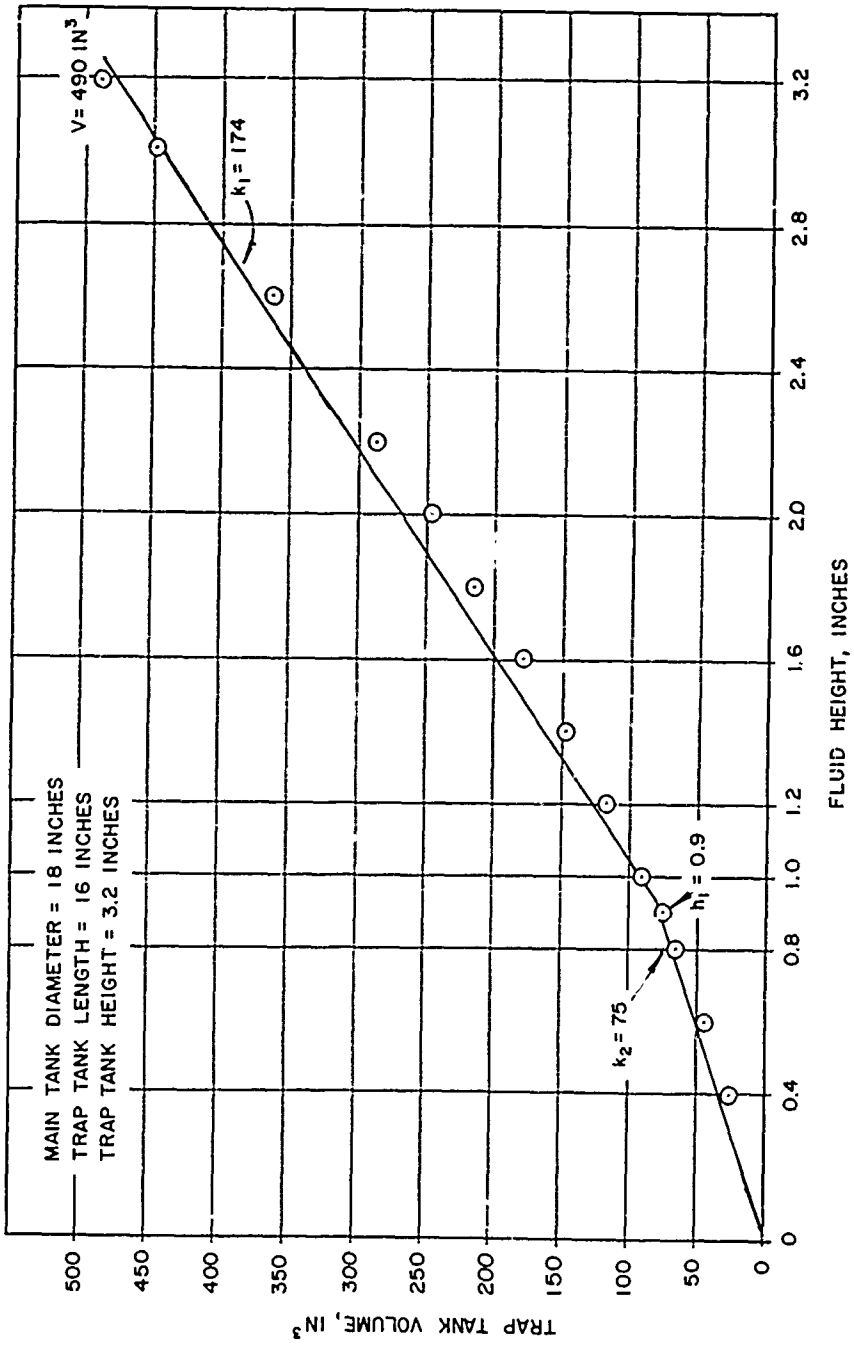

Figure 10. Trap Tank Fuel Volume Versus Fuel Height for 3.2 Inch Tank

Equation 26 is a general expression relating fuel height in the trap tank as a function of time. This analysis was primarily concerned with the total time required to empty the trap tank as a function of engine mass flow rate. An expression for maximum trap tank duration can be obtained by inserting the expression for linear function of height and volume (Equation 23) into the general relationship for trap tank duration (Equation 26) and by applying the boundary conditions that $t=t_{max}$ when $h = 0$. The resulting equation obtained is:

$$t_{max} = \frac{2}{\alpha} \left[k_1 \left(h_o^{1/2} - h_1^{1/2}\right) + k_2 h_1^{1/2}\right] + \frac{2Qe}{\alpha^2} \left[k_1 \ln \frac{(Qe + h_1^{1/2}\alpha)}{(Q_e + h_o^{1/2}\alpha)} + k_2 \ln \frac{(\quad Q_e \quad)}{(Q_e + h^{1/2}\alpha)}\right] \quad (33)$$

where, k_1 and k_2 = slopes of lines from either Figure 9 or 10

h_o = initial fluid height in tank, inches

h_1 = fluid height at point of slope change, inches

Equation 33 was programmed for solution by the Hewlett-Packard Model 9100 Calculator. For each run, all the terms on the right hand side of Equation 33 are input as constants including an initial value of engine mass flow rate ($\dot{m}$). The program then increments $\dot{m}$ by 0.5 and calculates t_{max} for each mass flow rate until the machine is stopped by the operator. Complete details of the computer program are described in the Appendix.

2. RESULTS FOR 9 INCH AND 3.2 INCH TRAP TANKS

Typical results are presented in Figures 11 through 17. Figure 11 shows the effect of orifice vent area for the 9-inch high by 9-inch long trap tank for a sustained load of negative ten g's. Orifice vent areas of 0.15 in^2, 0.20 in^2, and 0.25 in^2 were considered over a fuel flow rate range from 1.0 to 16 lb/sec. The retention times for these three orifice vent areas were significantly different from one another only at flow rates below 3.0 lb/sec. Above this flow rate the difference in retention time was less than one second. The other factor to be

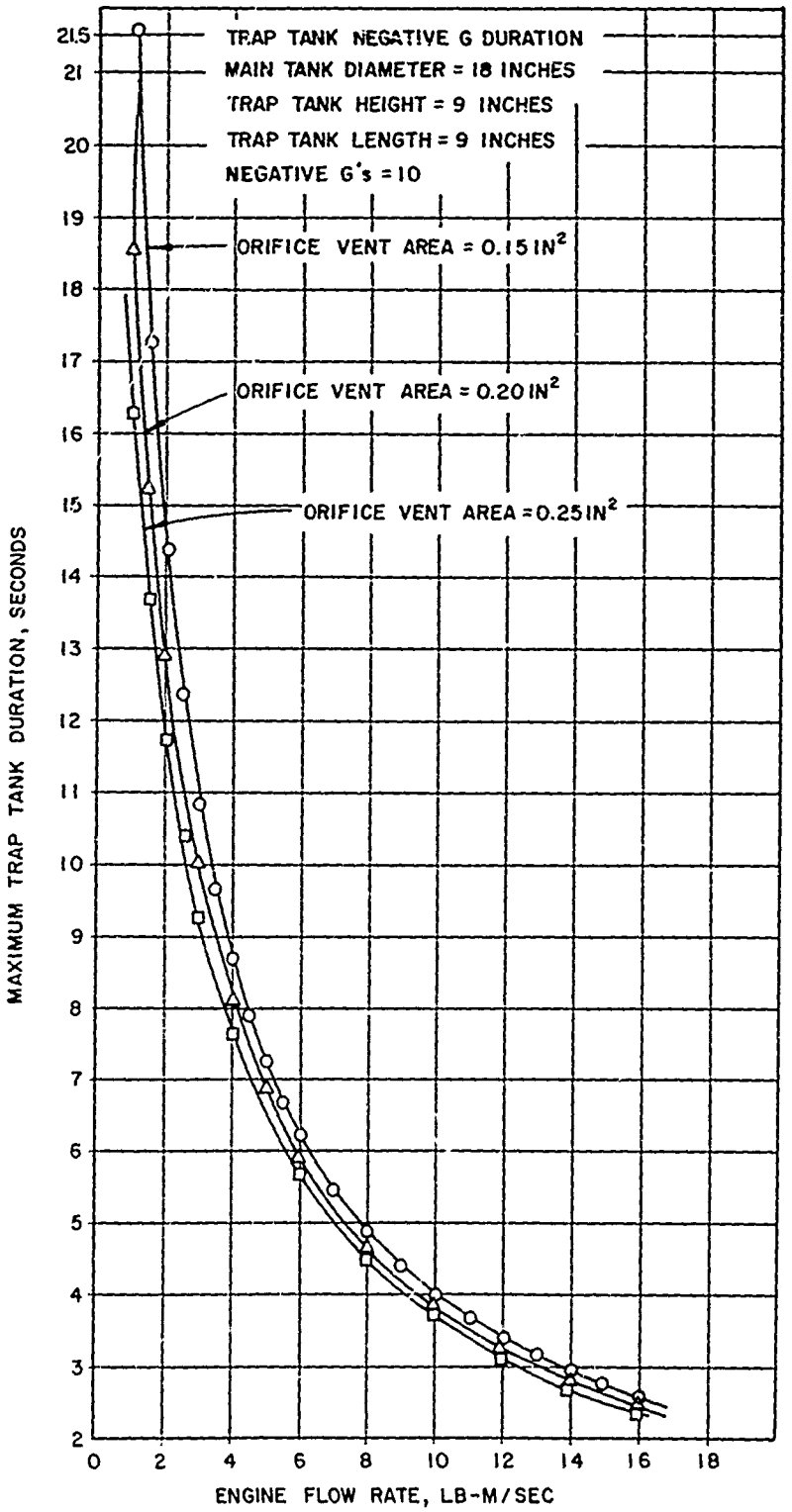

Figure 11. Tank Emptying Time, 9 Inch Height, 9 Inch Length, 10 G's, Various Vent Areas

considered is the total retention time obtained, regardless of orifice vent area considered, as a function of fuel flow rate to the engine. Figure 11 shows that the retention times for all three orifice vent areas decreases rapidly with increasing fuel flow rate. At 1.0 lb/sec engine flow rate the retention times range from 16.2 to 21.5 seconds. At 10 lb/sec engine flow rate the retention time was less than 4 seconds for all orifice vent areas.

The effect of acceleration (g) level on retention capability is shown in Figure 12. Acceleration levels of 1, 5, and 15 g's were evaluated with the nine inch high by nine inch long trap tank using an orifice vent area of 0.20 in^2. Again, as with the orifice vent area parameter, g level has a significant effect only at low flow rates. At flow rates above 4 lb/sec the difference in retention times for the 1 g and the 15 g cases is less than 2 seconds. For the 1 g case, retention time decreases rapidly from 18 seconds at 2 lb/sec to less than 4 seconds above 11 lb/sec flow rate. For the 15 g case, retention time at 2 lb/sec is only 11.5 seconds and rapidly decreases to under 4 seconds above fuel flow rates of 9 lb/sec.

The effect of trap tank size was examined by first decreasing tank height to 6 inches and maintaining the 9-inch tank length. Figure 13 shows the result of this change on retention time for the three orifice vent areas previously discussed and also at a 10 g acceleration level. For the 0.15 in^2 area at 1 lb/sec flow rate the retention time is 14 seconds versus 21.5 seconds for the 9 inch high trap tank. At 10 lb/sec the retention time for the 0.15 in^2 case is about 2.4 seconds. Similar decreases in retention time for the 0.20 in^2 and 0.25 in^2 orifice vent areas were obtained for the 6 inch high trap tank versus the 9 inch high trap tank.

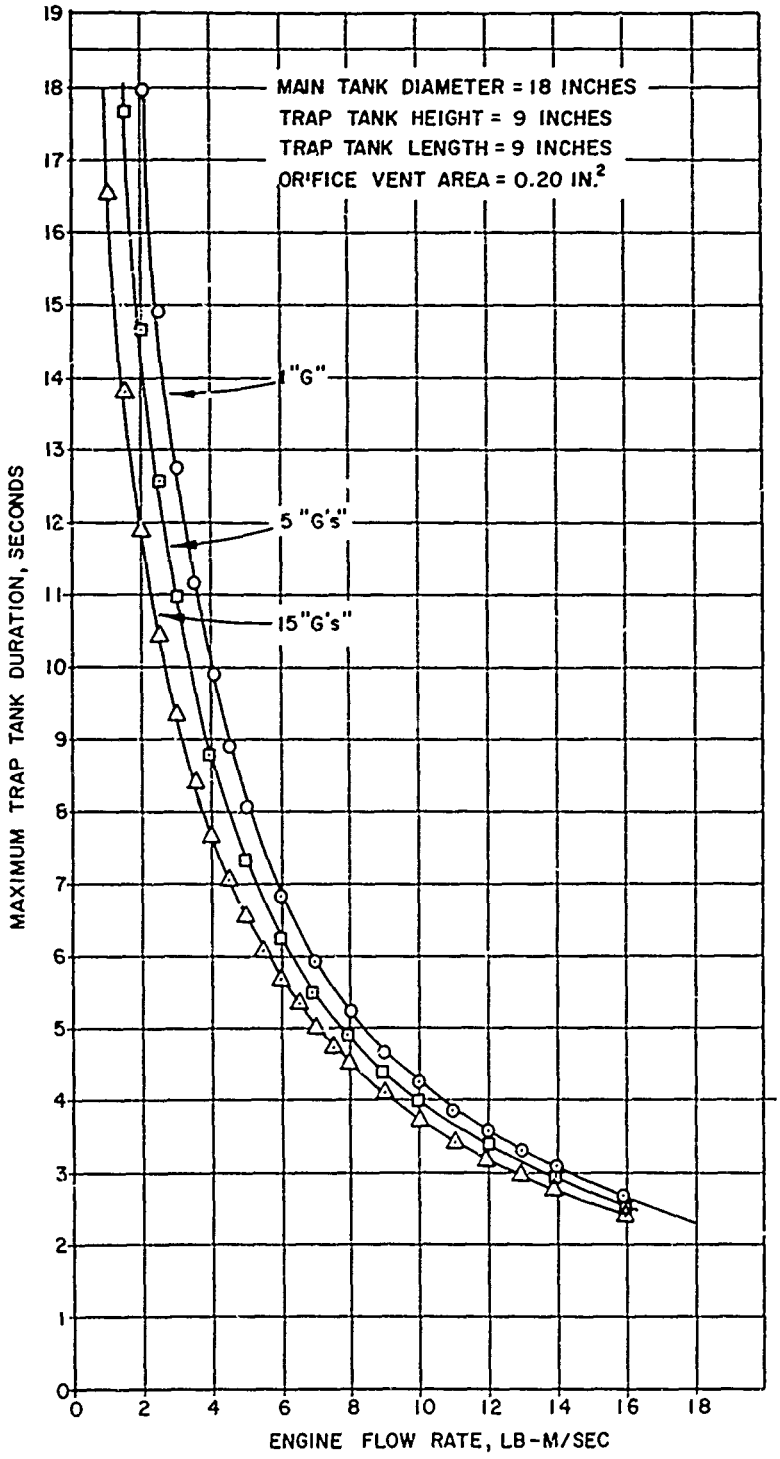

Figure 12. Tank Emptying Time, 9 Inch Height, 9 Inch Length, 0.20 In^2 Vent Area, Various G Levels

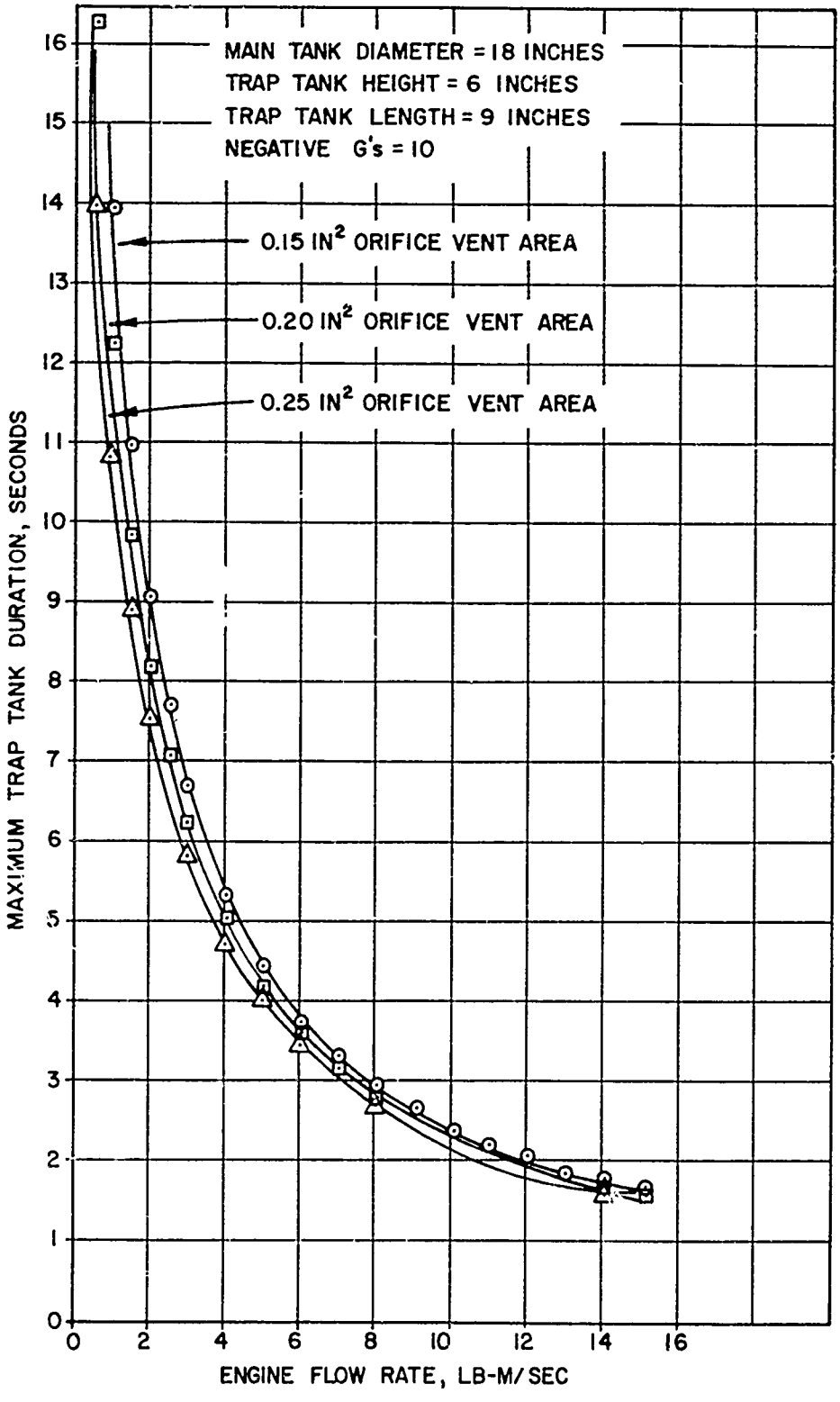

Figure 13. Tank Emptying Time, 6 Inch Height, 9 Inch Length, 10 G's, Various Vent Areas

Figure 14 presents the effect of g level on trap tank duration for the 6 inch high by 9 inch long trap tank. For this tank the effect of g level becomes important at fuel flow rates below 3 lb/sec. At this flow rate the difference in retention times between the 1 g case and the 15 g case is less than two seconds. Retention times at 1 lb/sec fuel flow rate ranged from 19 seconds for the 1 g case to 11 seconds for the 15 g case. At 10 lb/sec, retention time for both g levels was about 2.5 seconds.

The second variation made to change trap tank size was to increase length while maintaining the 9 inch height dimension. The same type of curves as before were obtained for the three orifice vent areas and for the three acceleration levels at a constant orifice vent area of 0.20 in^2. The primary effect was to increase retention time over the 9 inch length tank by a factor equal to the change in tank volumes. Data for the 12 inch length, 9 inch high trap tank are plotted in Figures 15 and 16.

Figure 17 presents retention time data for all three tanks having the common 9 inch height dimension. Tank lengths considered were 6, 9 and 12 inches. These calculations were made for the 10 g level using an orifice vent area of 0.20 in^2. The retention time versus flow rate curves obtained were the same type as before and the difference in retention times was a direct function of the tank length. Thus, the retention time for the 12 inch length tank at any fuel flow rate is very nearly twice the retention time for the 6 inch length tank. Retention time for the 12 inch length trap tank decreased from 32 seconds at a fuel flow rate of 0.5 lb/sec to about 5 seconds at 10 lb/sec flow rate whereas for the 6 inch tank length the retention time decreased from 16.6 seconds at 0.5 lb/sec flow rate down to about 2.6 seconds at 10 lb/sec flow rate.

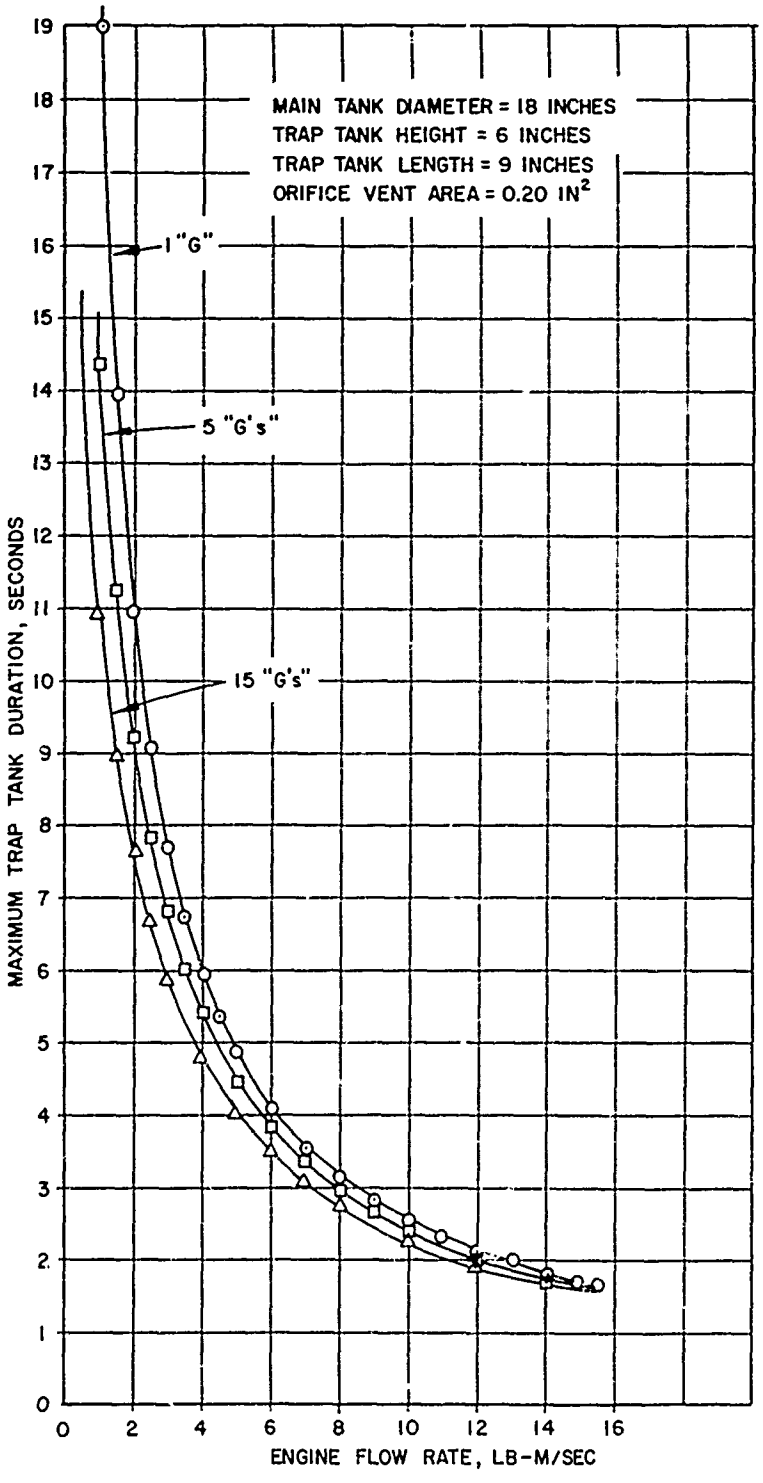

Figure 14. Tank Emptying Time, 6 Inch Height, 9 Inch Length, 0.20 In^2 Vent Area, Various G Levels

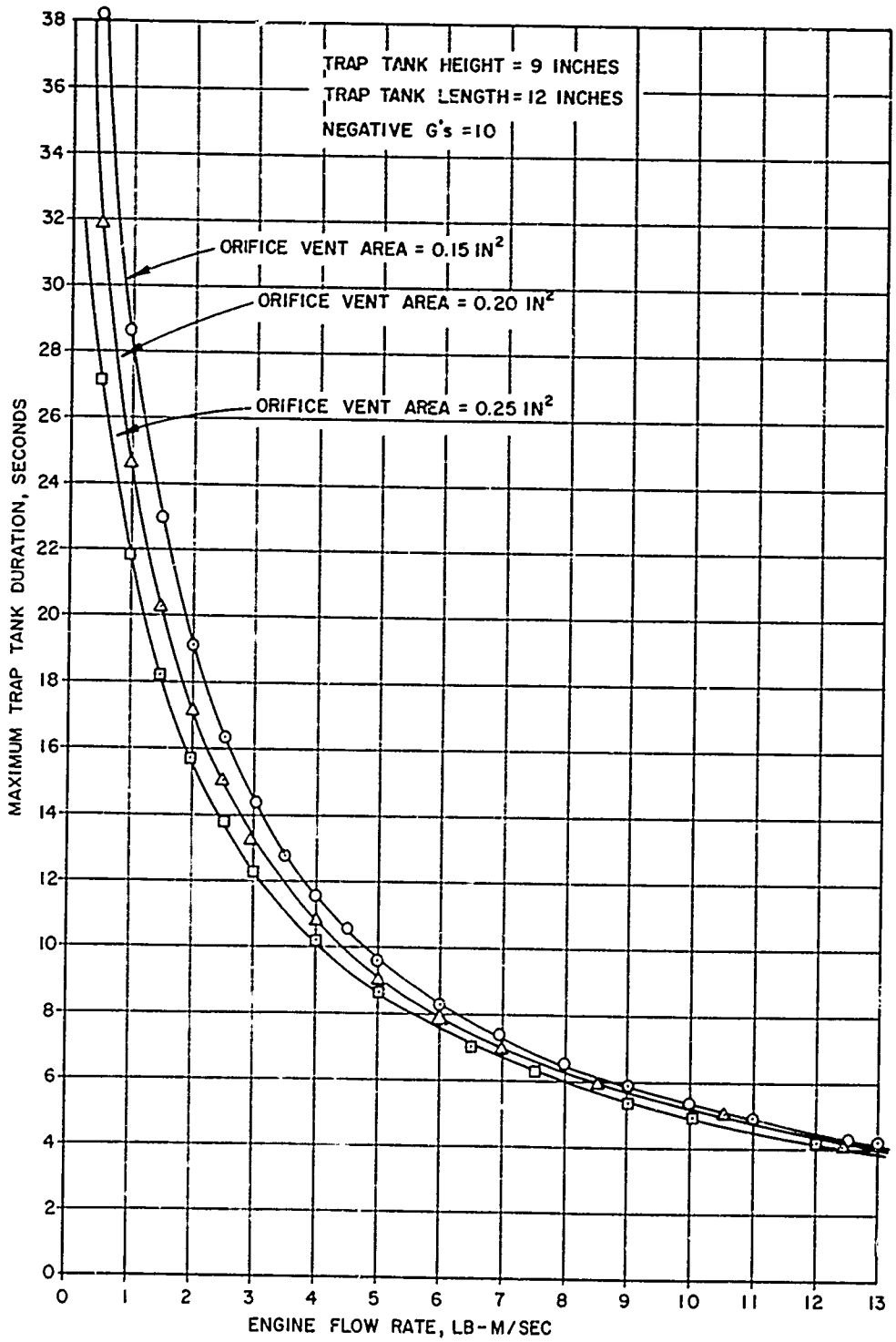

Figure 15. Tank Emptying Time, 9 Inch Height, 12 Inch Length, 10 G's Various Vent Areas

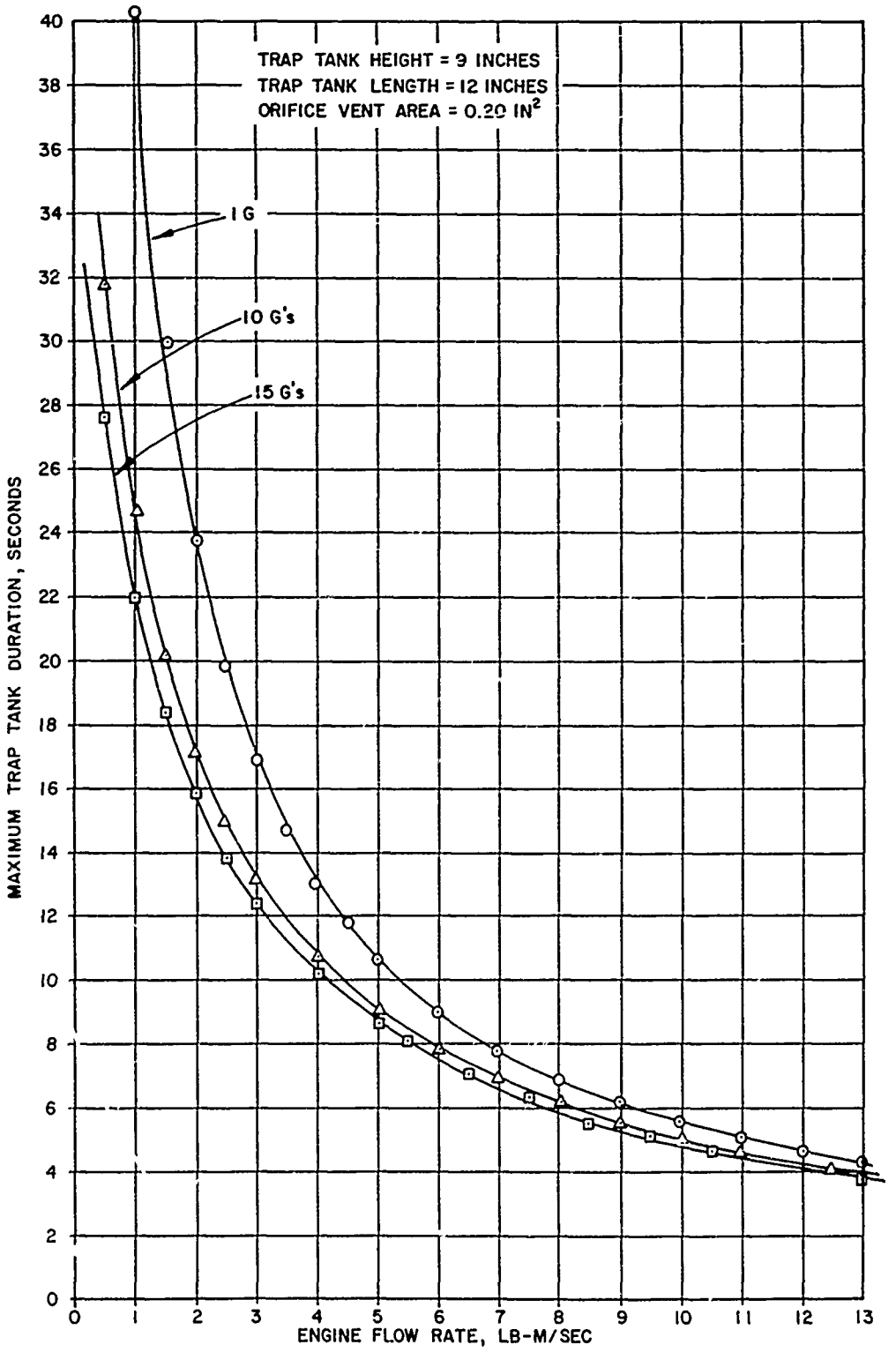

Figure 16. Tank Emptying Time, 9 Inch Height, 12 Inch Length, 0.20 In^2 Vent Area, Various G Levels

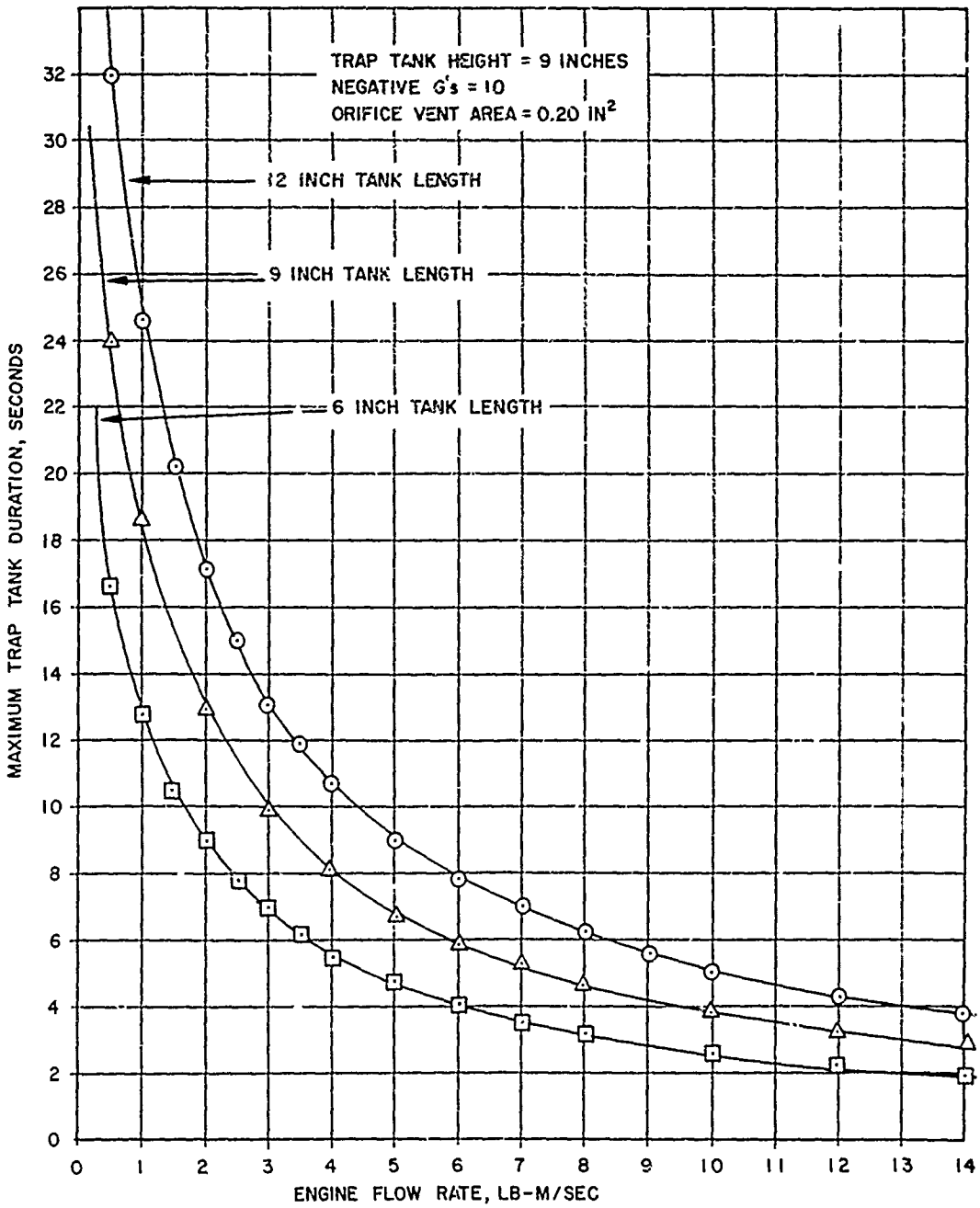

Figure 17. Tank Emptying Time, 9 Inch Height, 10 G's, 0.20 In^2 Vent Area, Various Tank Lengths

The dimensions and volumes of the four trap tanks considered so far by this analysis are as follows:

TABLE IV -- TRAP TANK VOLUMES

Trap Tank Dimensions	Volume, In^3
9-inch height, 6-inch length	763
9-inch height, 9-inch length	1145
9-inch height, 12-inch length	1527
6-inch height, 9-inch length	670

As shown by Figures 11 through 17, the retention times available with the four tanks listed in Table IV vary from over 40 seconds at fuel flow rates of 1.0 lb/sec and less to under three seconds for flow rates of 10 lbs/sec and over. Specific retention time available from a given trap tank will also depend on G level and orifice vent area as previously discussed. Fuel volume versus fuel height for the 3.2 inch high trap tank are presented in Table III and shown graphically in Figure 10. Maximum fuel volume for this trap tank is 490 in^3. Maximum trap tank retention times were calculated for this smaller tank using Equation 33. Figures 18 and 19 show the effect of orifice vent area at the 10 g acceleration level. Orifice vent areas used were 0.10 in^2, 0.15 in^2, 0.20 in^2, and 0.30 in^2. Again, the effect of orifice vent area was significant only at flow rates below 2 lb/sec. At 2 lb/sec the difference in retention time for the 0.10 in^2 case and 0.30 in^2 case was less than two seconds. As the flow rate was decreased toward zero the retention time difference for the two vent areas became significant whereas increasing flow rate above 2 lb/sec decreased the difference to an insignificant level.

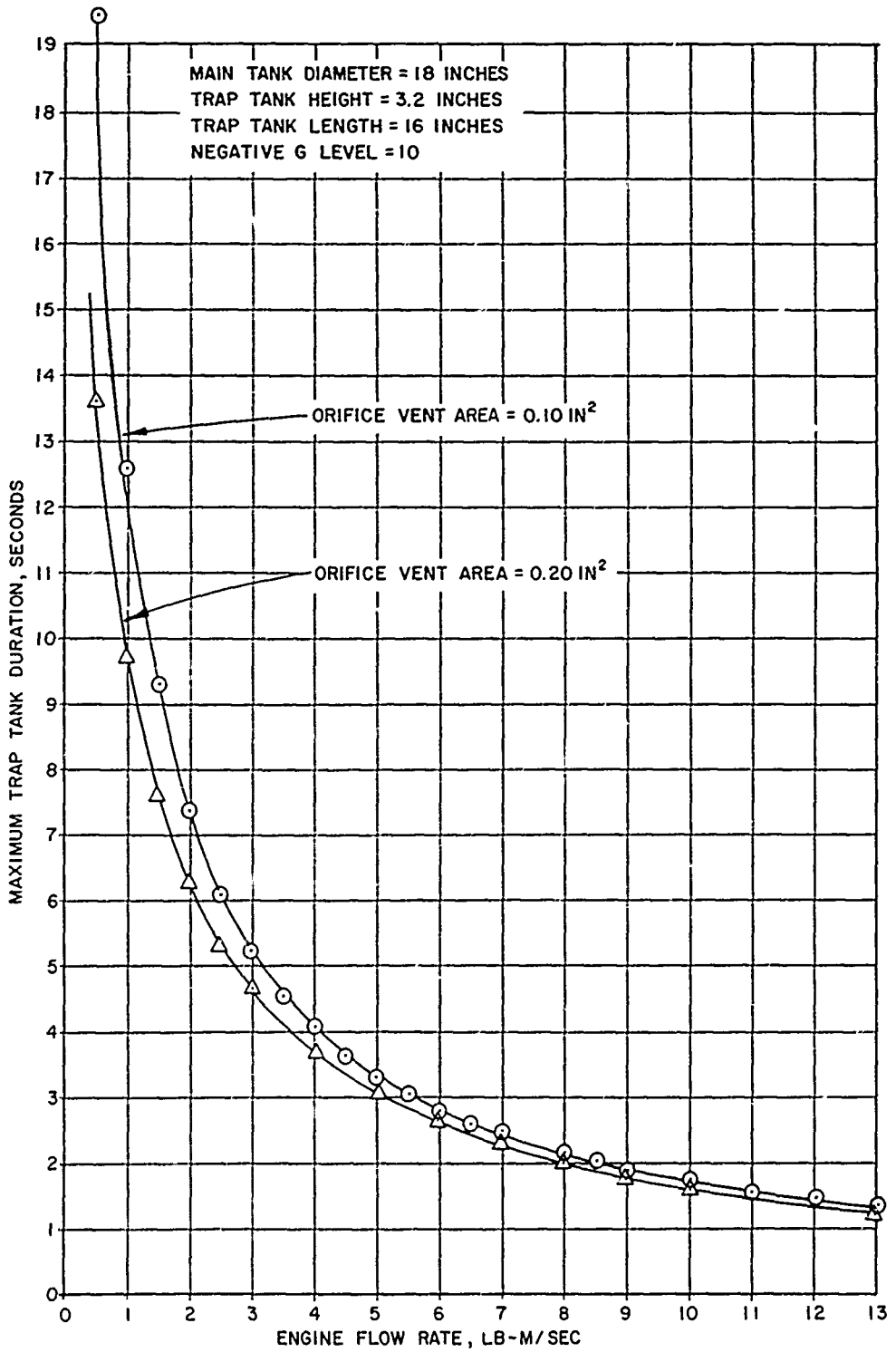

Figure 18. Tank Emptying Time, 3.2 Inch Height, 16 Inch Length, 10 G's, 0.10 and 0.20 In^2 Vent Areas

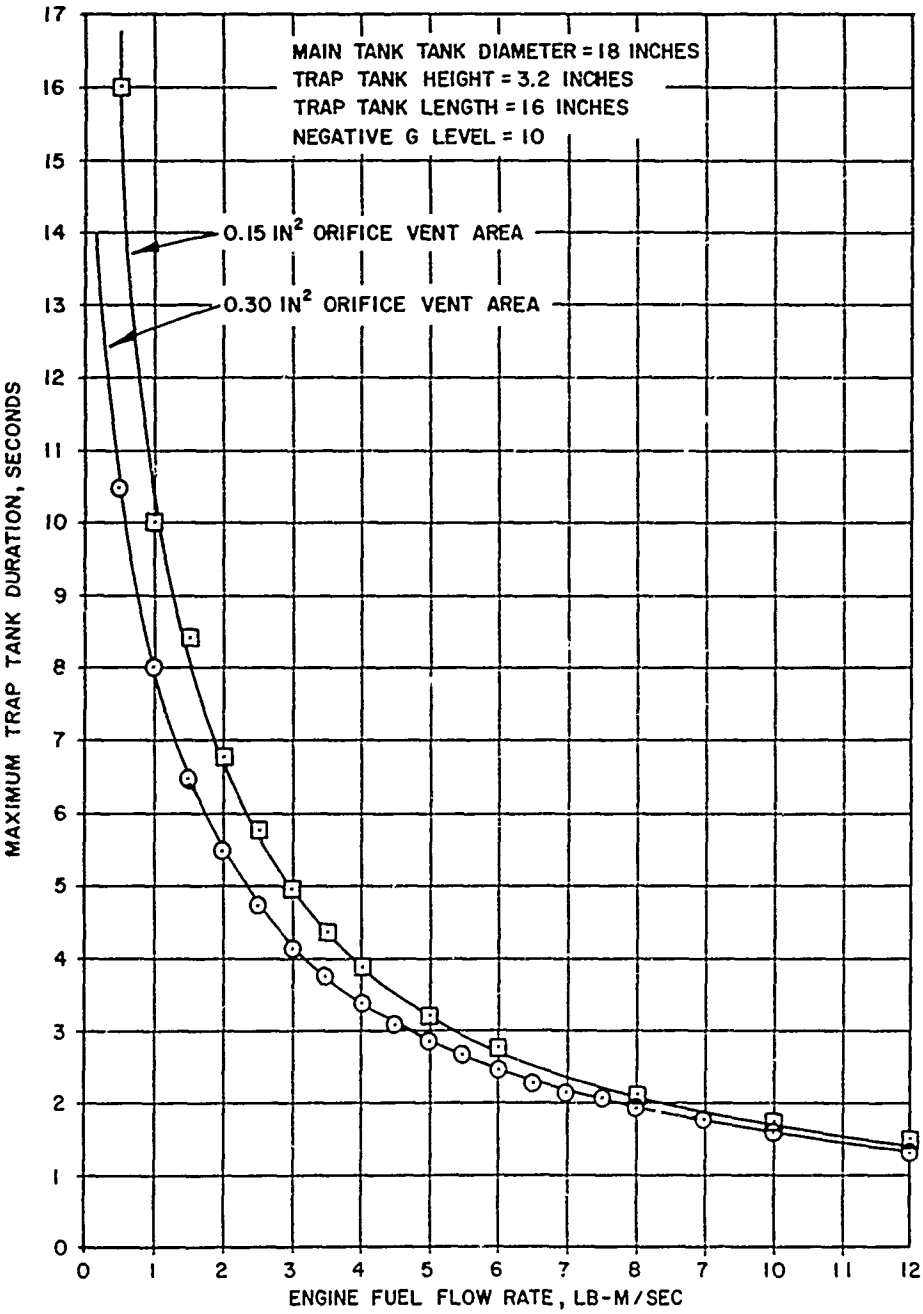

Figure 19. Tank Emptying Time, 3.2 Inch Height, 16 Inch Length, 10 G's, 0.15 and 0.30 In^2 Vent Areas

Figure 20 shows the effect of G level on retention time for the 3.2 inch high trap tank. Orifice vent area used was 0.20 in^2. Acceleration levels of 1, 5, and 20 g's were used to calculate retention time as a function of fuel flow rate to the engine. Once again, it is seen that acceleration level is significant only at relatively low mass flow rates. At 4 lb/sec the difference in retention times between the 1 g and the 20 g cases is less than one second but does increase to an appreciable difference at flow rates below 1.5 lb/sec. The retention time available with the 3.2 inch high trap tank vary from about 14 seconds with the 0.20 inch orifice vent area configuration at 1.0 lb/sec flow rate and 1 g to less than two seconds for all the conditions evaluated at flow rates above 9.0 lb/sec. These retention times are than about one-third of the 9 inch high trap tank values at 1.0 lb/sec flow rate and nearly the same values for flow rates above 10 lb/sec. These results can then be used to make a first estimate for trap tank size for a specific application. The critical factor is the retention time required at low flow rates since there exists a three-fold factor in retention times at 1.0 lb/sec for the two basic trap tank configurations considered. If retention times of less than 14 seconds at low flow rates are adequate, the 3.2 inch high trap tank would be the logical choice since this places less restrictions on the surface tension screen sizes, fuel temperatures, and acceleration levels which can be accommodated. At flow rates above 5.0 lb/sec the trap tank size becomes less critical with regard to retention time since the absolute values of the retention times is less than ten seconds and the maximum difference in retention times for the two primary configurations is less than 6 seconds.

The trap tank designs considered so far by this analysis have assumed that in the operational situation the axial g's are always unidirectional so that the trap tank can be located at one end of the main fuel tank. This would normally be the case for the climb and cruise segments of a missile trajectory where the acceleration force would keep the fuel at either the aft end and/or bottom of the main fuel tank. If missile maneuvering is required near the end of a mission when the main fuel tank is nearly empty the maneuvers would need to be restricted to those

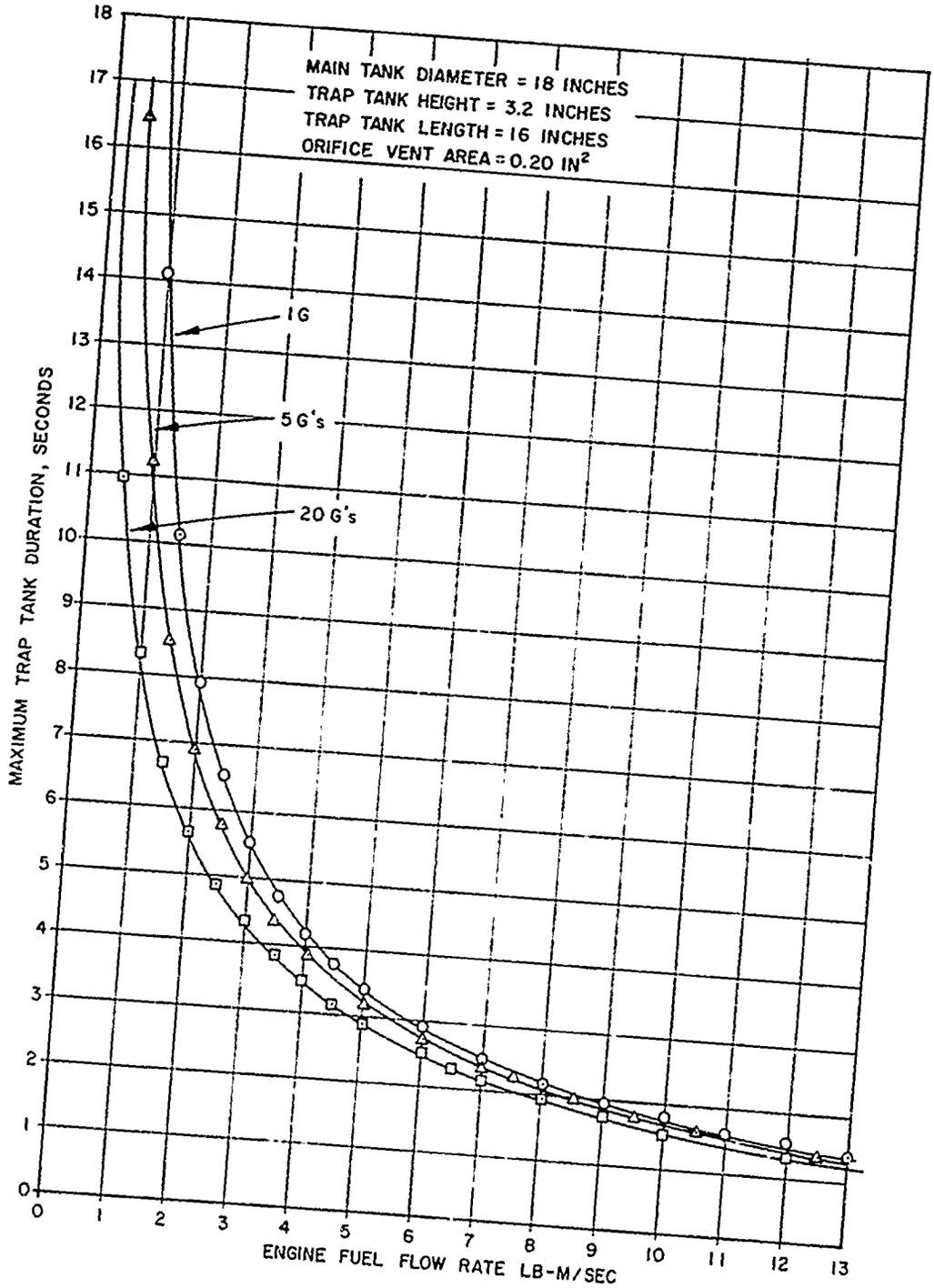

Figure 20. Tank Emptying Time, 3.2 Inch Height, 16 Inch Length, 0.20 In^2 Vent Area, Various G Levels

with a positive acceleration force in the direction of the trap tank. This restriction comes about due to the hydrostatic head limitation and configuration of the trap tank. Assuming that the maximum hydrostatic head which can be sustained is 3.2 inches of RJ-5, the location of the surface tension screen(s) inside the trap tank must be configured so that the 3.2 inch restriction is not exceeded during any missile maneuver. If this limit is exceeded, pressurant gas ingestion will occur the moment any portion of the surface tension screen becomes uncovered from the fuel.

SECTION IV

CONCLUSIONS AND RECOMMENDATIONS

Surface tension devices have been employed in a number of missiles and space vehicles to orient the fuel and to insure fuel flow during negative g maneuvers (Reference 1). Most of the applications to date have been for small (less than 1) negative g maneuvers and the fuel (or propellant) has been a low viscosity liquid. The analysis performed in this study considered much higher negative g levels than did previous applications of surface tension screens and also considered a fuel which is several orders of magnitude more viscous (at low temperatures) than the JP-type fuels or rocket propellants used in previous fuel systems. This extreme combination of a viscous fluid at a high negative g level make the use of surface tension devices impractical if not impossible. However, at low fuel flow rates and moderate (up to 3) negative g levels, surface tension devices may be applicable even with the viscous RJ-5 fuel. This would depend to a great extent on keeping the fuel temperature at a moderately high level, perhaps above 40°F as an example. This temperature restriction can be relieved by using a less viscous fuel such as the JP-9 type fuel currently being developed or by heating the RJ-5 fuel. If further analysis of the MPM reveals that operation in a low negative g environment is feasible, the utilization of surface tension screens may prove to be practicable.

APPENDIX

CALCULATION TECHNIQUE FOR TRAP TANK SIZING

The basic assumption used for the trap tank sizing analysis was that the fluid height remaining in the tank as a function of time is approximated by a linear relationship of the form:

$$V = a + kh \tag{34}$$

Differentiation of this equation and combination of the resulting differential equation with the expression for total volumetric flow rate out of the tank,

$$\frac{dV}{dt} = \frac{m}{\rho} + A\sqrt{2ghG} \tag{35}$$

produces the following expression for expulsion time:

$$t = \frac{2k}{\alpha}\left(h_o^{1/2} - h_1^{1/2}\right) + \frac{2kQe}{\alpha^2} \ln\left(\frac{Q_e + \alpha h_1^{1/2}}{Q_e + \alpha h_o^{1/2}}\right) \tag{36}$$

To obtain more nearly exact volumes as a function of fluid height, Equation 34 is evaluated over two segments as indicated by Figure 21. Total expulsion time then is,

$$t_{total} = t_1 + t_2 \tag{37}$$

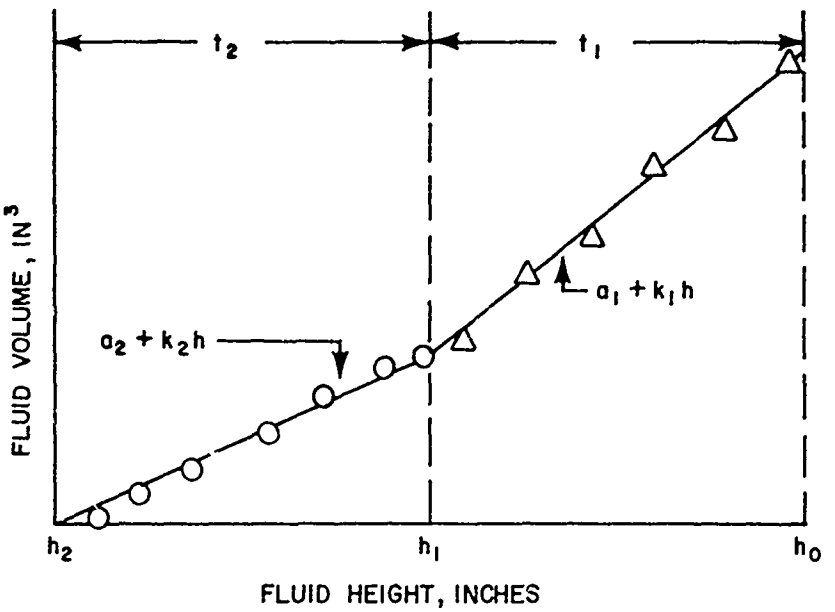

Figure 21. Fluid Volume Vs Fluid Height

The total expulsion time for each tank geometry is obtained by determining the two slopes (k_1 and k_2) of the linear approximation lines shown by Figure 21 while keeping the main tank diameter constant and using Equation 36 as follows:

$$t_1 = \frac{2k_1}{\alpha}\left(h_o^{1/2} - h_1^{1/2}\right) + \frac{2k_1 Q_e}{\alpha^2} \ln\left[\frac{Q_e + \alpha h_1^{1/2}}{Q_e + \alpha h_o^{1/2}}\right] \tag{38}$$

$$t_2 = \frac{2k_2}{\alpha}\left(h_1^{1/2} - h_2^{1/2}\right) + \frac{2k_2 Q_e}{\alpha^2} \ln\left[\frac{Q_e + \alpha h_2^{1/2}}{Q_e + \alpha h_1^{1/2}}\right] \tag{39}$$

Since h_2 approaches zero as the fluid volume approaches zero, Equation 39 reduces to:

$$t_2 = \frac{2k_2}{\alpha} h_1^{1/2} + \frac{2k_2 Q_e}{\alpha^2} \ln\left[\frac{Q_e}{Q_e + \alpha h_1^{1/2}}\right] \tag{40}$$

From Equation 37,

$$t_{total} = t_{max} = t_1 + t_2 \tag{41}$$

Substituting Equations 38 and 40 into Equation 41 and simplifying gives:

$$t_{max} = \frac{2}{\alpha}\left[K_1(h_0^{\frac{1}{2}} - h_1^{\frac{1}{2}}) + K_2 h_1^{\frac{1}{2}}\right] + \frac{2Q_e}{\alpha^2}\left[K_1 \ln\left(\frac{Q_e + \alpha h_1^{\frac{1}{2}}}{Q_e + \alpha h_0^{\frac{1}{2}}}\right) + K_2 \ln\left(\frac{Q_e}{Q_e + \alpha h_1^{\frac{1}{2}}}\right)\right] \tag{42}$$

where $\alpha = A\sqrt{2g_c G} = A\sqrt{772.8G}$

$Q_e = \frac{\dot{m}}{\rho}$

All terms on right hand side of Equation 42 can be input as constants for one run including initial value of $\dot{m}$. $\dot{m}$ is incremented for each time calculation by adding 0.5. Program will continue to calculate t_{max} for each $\dot{m}$ until machine is stopped by operator.

Program 1 and Program 2 are recorded on a magnetic card for reuse.

Before executing program, store values in registers:

$A \rightarrow 201$

$G \rightarrow 202$

$h_{o_1} \rightarrow 203$

$k_1 \rightarrow 204$

$k_2 \rightarrow 205$

$h_1 \rightarrow 206$

$\rho \rightarrow 207$

$\dot{m} \rightarrow 200$ (initial value)

PROCEDURE

1. Store constants in registers as on previous page
2. Put Program 1 and Program 2 in extended memory
3. Turn on printer with "X" key depressed
4. Press 1, FMT, GO TO, CONTINUE
5. Program will continue until operator presses STOP

ADDITIONAL CASES

1. Enter any new constants in registers
   NOTE: Reset initial value of $\dot{m}$
2. Start with instruction 4 above

OUTPUT FORMAT

SEE RIGHT

1) The program first outputs the initial constants stored in the registers.

$A = 0.20$

$G = 1.0$

$h_{o_1} = 9.0$

$h_1 = 3.0$

$k_1 = 200$

$k_2 = 100$

$\rho = 0.46$

2) Then values of $\dot{m}$ and its corresponding t are printed as the program continues to increment $\dot{m}$ and solve for t.

$\dot{m} = 0.5$

$t = 130.323-$

$\dot{m} = 1.0$

$t = 116.557$

$\dot{m} = 1.5$

$t = 106.121$

Title Program 1

HEWLETT · PACKARD

Step	Key	Code	Display x	Display y	Display z
00	CLEAR				
01	2				
02	0				
03	1				
04	FMT				
05	π				
06	PRINT				
07	2				
08	0				
09	2				
0a	FMT				
0b	π				
0c	PRINT				
0d	2				

HEWLETT · PACKARD

Step	Key	Code	Display x	Display y	Display z
10	0				
11	3				
12	FMT				
13	π				
14	PRINT				
15	2				
16	0				
17	6				
18	FMT				
19	π				
1a	PRINT				
1b	2				
1c	0				
1d	4				

HEWLETT PACKARD

Step	Key	Code	Display x	Display y	Display z
20	FMT				
21	π				
22	PRINT				
23	2				
24	0				
25	5				
26	FMT				
27	π				
28	PRINT				
29	2				
2a	0				
2b	7				
2c	FMT				
2d	π				

HEWLETT · PACKARD

Step	Key	Code	Display x	Display y	Display z
30	PRINT				
31	PRINT				
32	PRINT				
33	PRINT				
34	2				
35	FMT				
36	GOTO				
37	CLEAR				
38	2				
39	0				
3a	3				
3b	FMT				
3c	π				
3d	$\sqrt{x}$				

HEWLETT · PACKARD

Step	Key	Code	Display x	Display y	Display z
40	+				
41	2				
42	0				
43	6				
44	FMT				
45	π				
46	$\sqrt{x}$				
47	−				
48	2				
49	0				
4a	4				
4b	FMT				
4c	π				
4d	x				

HEWLETT · PACKARD

Step	Key	Code	Display x	Display y	Display z
50	2				
51	0				
52	6				
53	FMT				
54	π				
55	$\sqrt{x}$				
56	+				
57	2				
58	0				
59	5				
5a	FMT				
5b	π				
5c	x				
5d	+				

Step	Key	Code	Display x	Display y	Display z
60	+				
61	2				
62	x				
63	b				
64	÷				
65	2				
66	0				
67	8				
68	FMT				
69	π				
6a	+			ANS	
6b	2				
6c	0				
6d	0				

Step	Key	Code	Display x	Display y	Display z
70	FMT				
71	π		ṁ		
72	PRINT				
73	x⇄y				
74	PRINT		ANS	ṁ	
75	PRINT				
76	.				
77	5				
78	+				
79	2				
7a	0				
7b	0				
7c	FMT				
7d	y→( )				

Storage

f	
e	
d	
c	
b	
a	
9	
8	
7	
6	
5	
4	
3	
2	
1	
0	

Title Program 1 (cont.)

Step	Key	Code	Display x	Display y	Display z	Step	Key	Code	Display x	Display y	Display z	Step	Key	Code	Display x	Display y	Display z
0	GO TO					0						0					
1	3					1						1					
2	4					2						2					
3	END					3						3					
4						4						4					
5						5						5					
6						6						6					
7						7						7					
8						8						8					
9						9						9					
a						a						a					
b						b						b					
c						c						c					
d						d						d					
0						0						0					
1						1						1					
2						2						2					
3						3						3					
4						4						4					
5						5						5					
6						6						6					
7						7						7					
8						8						8					
9						9						9					
a						a						a					
b						b						b					
c						c						c					
d						d						d					
0						0						Storage					
1						1						f					
2						2						e					
3						3						d					
4						4						c					
5						5						b					
6						6						a					
7						7						9					
8						8						8					
9						9						7					
a						a						6					
b						b						5					
c						c						4					
d						d						3					
												2					
												1					
												0					

Title Program 2 (Subroutine)

HEWLETT · PACKARD

Step	Key	Code	Display x	Display y	Display z
00	CLEAR				
01	2				
02	0				
03	0				
04	FMT				
05	π				
06	↑				
07	2				
08	0				
09	7				
0a	FMT				
0b	π				
0c	÷				
0d	y→()				

HEWLETT · PACKARD

Step	Key	Code	Display x	Display y	Display z
10	a				
11	7				
12	7				
13	2				
14	.				
15	8				
16	↑				
17	2				
18	0				
19	2				
1a	FMT				
1b	π				
1c	x				
1d	↓				

HEWLETT · PACKARD

Step	Key	Code	Display x	Display y	Display z
20	x				
21	↑				
22	2				
23	0				
24	1				
25	FMT				
26	π				
27	x				
28	y→()				
29	b				
2a	2				
2b	0				
2c	6				
2d	FMT				

Step	Key	Code	Display x	Display y	Display z
30	π				
31	x				
32	x				
33	a				
34	+				
35	y→()				
36	d				
37	b				
38	↑				
39	2				
3a	0				
3b	3				
3c	FMT				
3d	π				

Step	Key	Code	Display x	Display y	Display z
40	x				
41	x				
42	a				
43	+				
44	↓				
45	÷				
46	↓				
47	ln x				
48	↑				
49	2				
4a	0				
4b	4				
4c	FMT				
4d	π				

Step	Key	Code	Display x	Display y	Display z
50	X				
51	y→()				
52	c				
53	d				
54	↑				
55	a				
56	x⇄y				
57	÷				
58	↓				
59	ln x				
5a	↑				
5b	2				
5c	0				
5d	5				

Step	Key	Code	Display x	Display y	Display z
60	FMT				
61	π				
62	x				
63	c				
64	+				
65	a				
66	x				
67	2				
68	x				
69	b				
6a	÷				
6b	÷				
6c	2				
6d	0				

Step	Key	Code	Display x	Display y	Display z
70	8				
71	FMT				
72	y→()				
73	FMT				
74	END				
75					
76					
77					
78					
79					
7a					
7b					
7c					
7d					

Storage

f	
e	
d	
c	
b	
a	
9	
8	
7	
6	
5	
4	
3	
2	
1	
0	

REFERENCES

1. Heller, William and Cadwallader, E. A., Positive Expulsion-State of the Art Study, Chemical Propulsion Information Agency, The Johns Hopkins University, Applied Physics Laboratory, Silver Spring MD, CPIA Publication 210, May 1971.

2. Braendlein, R. K., Fuel Expulsion Test Evaluation and Design Parameters, P. D. Study 51-2054, The Marquardt Company, Van Nuys CA, February 1972.

3. Vought Missiles and Space Company, Harpoon Missile Fuel System-Supplementary Analysis and Test Data, VMSC Report No. TP130 RP-L-10211, 8 March 1971.

4. Perry, John H. (editor), "Chemical Engineers Handbook", Fourth Edition, Page 5 - 35.

5. Armour, James C. and Cannon, Joseph H., "Fluid Flow Through Woven Screens", Journal of the American Institute of Chemical Engineers, Volume 14, No. 3.

6. Orton, G. F., Harpoon Surface Tension Fuel Acquisition System, McDonnell Douglas Astronautics Company, Memo No. EM-1-E243-12, 21 July 1971.

7. Orton, G. F., Screen Properties for Surface Tension Fuel Acquisition Systems, McDonnell Douglas Astronautics Company, Telecon Report dated 22 February 1973.

8. Tucker, R. H., The Development and Verification of Theoretical Models for the Performance of Wire Filter Media, Thesis, Oklahoma State University, July 1966.